An overview of the Lagrangian experiments undertaken during the North Atlantic regional Aerosol Characterisation Experiment (ACE-2)

Doug W. Johnson, Simon Osborne, Robert Wood, Karsten Suhre, Randy Johnson, Steven Businger, Patricia K. Quinn, Alfred Wiedensohler, Philip A. Durkee, Lynn M. Russell, Meinrat O. Andreae, Colin O'Dowd, Kevin J. Noone, Brian Bandy, J. Rudolph & Spyros Rapsomanikis

An overview of the Lagrangian experiments undertaken during the North Atlantic regional Aerosol Characterisation Experiment (ACE-2)

By DOUG W. JOHNSON[1]*, SIMON OSBORNE[1], ROBERT WOOD[1], KARSTEN SUHRE[2], RANDY JOHNSON[3], STEVEN BUSINGER[4], PATRICIA K. QUINN[5], ALFRED WIEDENSOHLER[6], PHILIP A. DURKEE[7], LYNN M. RUSSELL[8], MEINRAT O. ANDREAE[9], COLIN O'DOWD[10], KEVIN J. NOONE[11], BRIAN BANDY[12], J. RUDOLPH[13] and SPYROS RAPSOMANIKIS[14], [1]*Met. Research Flight, Building Y46, DERA, Farnborough, Hants, UK;* [2]*CNRM, University of Toulouse, France;* [3]*NOAA, ARL, Idaho Falls, USA;* [4]*University of Hawaii, USA;* [5]*PMEL, NOAA, Seattle, USA;* [6]*IFT, Leipzig, Germany;* [7]*CIRPAS, NPS, Monterey, USA;* [8]*Princeton University, USA;* [9]*MPI for Chemistry, Mainz, Germany;* [10]*CMAS, University of Sunderland, UK;* [11]*MISU, University of Stockholm, Sweden;* [12]*University of East Anglia, UK;* [13]*University of York, Canada;* [14]*Demokritos University of Thrace, Greece*

ABSTRACT

One of the primary aims of the North Atlantic regional Aerosol Characterisation Experiment (ACE-2) was to quantify the physical and chemical processes affecting the evolution of the major aerosol types over the North Atlantic. The best, practical way of doing this is in a Lagrangian framework where a parcel of air is sampled over several tens of hours and its physical and chemical properties are intensively measured. During the intensive observational phase of ACE-2, between 15 June 1997 and 24 July 1997, 3 cloudy Lagrangian experiments and 3 cloud-free, Lagrangian experiments were undertaken between the south west tip of the Iberian Peninsula and the Canary Islands. This paper gives an overview of the aims and logistics of all of the Lagrangian experiments and compares and contrasts them to provide a framework for the more focused Lagrangian papers in this issue and future process modelling studies and parametrisation development. The characteristics of the cloudy Lagrangian experiments were remarkably different, enabling a wide range of different physical and chemical processes to be studied. In the 1st Lagrangian, a clean maritime air mass was sampled in which salt particle production, due to increased wind speed, dominated the change in the accumulation mode concentrations. In the 2nd Lagrangian, extensive cloud cover resulted in cloud processing of the aerosol in a polluted air mass, and entrainment of air from the free troposphere influenced the overall decrease in aerosol concentrations in the marine boundary layer (MBL). Very little change in aerosol characteristics was measured in the 3rd Lagrangian, where the pollution in the MBL was continually being topped up by entraining air from a residual continental boundary layer (CBL) above. From the analysis of all the Lagrangian experiments, it has been possible to formulate, and present here, a generalised description of a European continental outbreak of pollution over the sub-tropical North Atlantic.

---

* Corresponding author address: Meteorological Research Flight, Building Y46, DERA, Farnborough, Hants, GU14 0LX, UK.
e-mail: dwjohnson@meto.gov.uk

1. Introduction

The 1995 IPCC report highlights the fact that the current estimates of the global mean radiative forcing due to anthropogenic aerosol are highly variable (-0.3 to -3.5 W m^{-2}) and of a comparable magnitude but opposite sign to the forcing due to anthropogenic CO_2 and the other greenhouse gases (Charlson et al., 1991, 1992; Kiehl and Briegleb, 1993; Penner et al., 1994). Considering the potential importance of aerosol forcing it is remarkable how many global climate models ignore the effects of aerosol and in the case of the rest how poorly they parametrise their effects. This is primarily due to the lack of both globally distributed data and a clear understanding of the processes that link gaseous precursor emissions, atmospheric aerosol properties and their direct and indirect radiative effects. Thus to obtain more accurate climate model predictions it is imperative that attention be focused on quantifying the processes controlling the natural and anthropogenic aerosol and on minimising the uncertainties in the calculated climate forcing.

The intensive observational phase of the North Atlantic regional Aerosol Characterisation Experiment (ACE-2) (Raes et al., 2000) was undertaken in June and July 1997. One of the major projects of ACE-2 was to study the evolution of continental air masses in the marine environment and to understand the processes that dominate that evolution. The only effective way of doing this is in a Lagrangian framework. It is extremely difficult to interpret from a Eulerian approach how the aerosol characteristics of a parcel of air are modified in time. Therefore it is necessary to follow a parcel of air making measurements in it continuously, or as often as possible, over an extended period. The major objective of these Lagrangian experiments was to follow outbreaks of European continental air as they were advected south westwards in the trade winds through the sub-tropical North Atlantic and to investigate using aircraft measurements how the aerosol characteristics and their effects on clouds evolve with time. Using this approach ensures that the observed changes are only due to chemical and physical processing and not due to advection and changing air mass.

The Lagrangian approach attempted here was first developed for measuring atmospheric oxida-

tion processes and chemical budgets during the Atlantic Stratocumulus Transition Experiment (ASTEX, Huebert et al., 1996). The technique relies on being able to track a parcel of air over several hours or days. This is achieved by tagging the air parcel using constant level balloons (Businger et al., 1996) which have GPS receivers and can transmit their positions to within a few hundred meters. In ASTEX, the balloons' ability to stay at constant altitude was severely restricted whenever it got wet through entering cloud or drizzle and its buoyancy decreased, often resulting in it entering the sea. The strategy was further developed during the Aerosol Characterisation Experiment (ACE-1, Bates et al., 1998) where "smart" balloons (Businger et al., 1999) were used. Their buoyancy could be adjusted by pumping or removing air from an internal bladder in order to maintain a constant altitude. The balloons used during ACE-2 had the added advantage that their buoyancy could be modified in flight by an operator in the tracking aircraft (Johnson and Businger, 2000).

The main aim of the Lagrangian experiments was to satisfy the second objective of ACE-2 (Raes et al., 2000), i.e., to quantify the physical and chemical processes controlling the evolution of the major aerosol types and in particular their physical, chemical, radiative and cloud nucleating properties. However, as measurements have been made which characterise the physical, chemical, radiative and cloud nucleating properties of the aerosol in the air parcel being followed, objective 1 is also directly satisfied. In the longer term it is hoped that the understanding about aerosol processes gained through the integration of the analysis of the Lagrangian measurements with the analysis from other ACE-2 projects, e.g., HILLCLOUD (Bower et al., 2000) and FREETROPE will indirectly, through parametrisation development, numerical modelling and extrapolation of satellite observations, be used to assess the regional direct and indirect radiative forcing of aerosol and thus help attain objective 3.

2. Scientific rationale

Our inability to model and predict climate change comes about through a lack of understanding of the processes governing the interactions

between clouds, aerosols and atmospheric chemistry. The ACE-2 Lagrangian experiments tried to improve this position by producing a data set that has a diverse and complete enough set of measurements whereby through a combination of data interpretation, process model simulation, and model parametrisation development the important processes can be identified and understood.

The processes that govern the number size distribution and size dependent chemical composition of the aerosol in a parcel of air and hence its radiative impact are qualitatively known. They include the following.

  (i) Homogeneous gas phase chemistry.
 (ii) New particle formation by multi-component homogeneous nucleation.
(iii) Condensation on aerosol.
 (iv) Aerosol coagulation.
  (v) Dry deposition of aerosol.
 (vi) Cloud processing of aerosol, including, droplet activation, in-cloud chemistry, droplet coalescence, scavenging of aerosol by droplets, droplet evaporation, and precipitation.
(vii) Meteorology

These processes will compete when a continental air mass is advected over the sea. The rates of some of the individual processes have been investigated in the laboratory and parametrised in process models. However, predictions of such models, even when applied to the simple case of the minimally polluted MBL, disagree strongly about the importance of individual processes (Pandis et al., 1994; Raes, 1995). Thus observations in the atmosphere are required to verify whether the processes that are presently accounted for in the models are sufficient, and to develop improved aerosol parametrisations. The platforms involved in the Lagrangian experiments were comprehensively instrumented (details in Section 4) to optimise our ability to determine the processes operating; in particular, cloud processing, mixing with the free troposphere, and changes in the accumulation mode and CCN characteristics (e.g., sea spray emissions). One of the difficulties in studying aerosol processes is accounting for the highly coupled nature of the aerosol, cloud and meteorological processes. It is therefore practical to distinguish between processes in the cloud-free and cloudy parts of the atmosphere.

2.1. Processes in a cloud-free atmosphere

The aerosol concentration in a continental air mass advecting in a cloud-free MBL will be depleted mainly by dry deposition, horizontal dispersion and exchange between the MBL and free troposphere. During ASTEX the latter was found to be important (Zhuang and Huebert, 1996). However, exchange with the free troposphere may also be a source of aerosol in the MBL when a more highly polluted continental air mass is transported over the area in the free troposphere, e.g., a Saharan dust outbreak. Thus aerosol profiles across the top of the MBL and accurate entrainment rates must be quantified to close the aerosol mass and number balance of the MBL (Russell et al., 1998; Van Dingenen et al., 1999). Presently, entrainment rates have been estimated only within a factor of 2 (Bretherton, 1995; Russell et al., 1998) and so multiple redundant measurement techniques have been used during the Lagrangian experiments (Sollazzo et al., 2000) to improve these estimates.

For aerosol species like black carbon and mineral dust, changes in the aerosol size distribution in the MBL will be indicative of entrainment, and removal only. However, sulphate will be chemically produced over the oceans from SO_2 in the anthropogenic plume and from oceanic DMS. Homogeneous nucleation of precursors has been observed in the MBL (Covert et al., 1992) and does increase the number concentration. However its occurrence is subject to a variety of conditions such as pre-existing aerosol surface area, which act as a sink for the precursor gases and preclude nucleation. Highly polluted continental plumes may well provide enough aerosol surface area to restrict new nucleation. Similarly, in high wind situations, salt particle production from sea spray may produce a large enough particle surface area to be a sink for sulphur species in the MBL (Sievering et al., 1992; Suhre et al., 1995). It has been assumed that sea spray produces large ($>1\,\mu m$) particles that have too short residence times to act as CCN (Charlson et al., 1987). However, recent observations have re-opened the debate about the rôle of sea salt particles in the aerosol and cloud condensation nuclei (CCN) number concentration (O'Dowd et al., 1993; Murphy et al., 1998) and the measurements made in ACE-2 have reiterated this (Johnson et al.,

2000). To obtain reliable rates for production, transformation and removal of aerosol, the mass and number balances of the major aerosol components that were advected from the continent or were produced in situ have been measured during ACE-2 using filter samples, and optical probes to determine the change in aerosol size spectra over a wide range of sizes. Similarly, the rôle of coagulation, condensational growth and dry deposition can be studied by measuring the evolution of the number size distribution down to the nanometre range.

2.2. Processes in a cloudy atmosphere

A variety of processes induced by clouds can affect the aerosol mass and number concentration. The in-cloud oxidation of SO_2 is a major pathway for producing sulphate mass in the global atmosphere (Hegg, 1985; Langner and Rodhe, 1991; Benkovitz et al., 1994). There are however large uncertainties concerning the oxidation efficiencies which may account for a factor of 2 uncertainty in the estimates of the global direct forcing of sulphate aerosols (Kiehl and Rodhe, 1995). The Lagrangian experiments and HILLCLOUD (Bower et al., 2000) have attempted to make a more accurate determination of this by measuring O_3, H_2O_2, cloud liquid water content and cloud droplet size spectrum, in combination with predictions from an explicit cloud microphysics model (Dore et al., 2000).

Processes such as droplet coalescence and scavenging of interstitial particles by cloud droplets affect the aerosol and CCN number budget. Coalescence will reduce particle concentrations in the MBL but increase particle sizes (Feingold et al., 1996), thereby improving their CCN characteristics. Scavenging of interstitial aerosol by cloud droplets will reduce particle concentrations in the MBL and modify the CCN supersaturation spectra. These processes, together with precipitation, play a major rôle in transforming the continental air mass advecting within the MBL into a maritime air mass. A time-scale analysis of the relative contribution of these and other processes to the transformation is presented in Hoell et al. (2000).

Recent measurements have shown that clouds may also be the source of particles through homogeneous nucleation that is promoted by high relative humidity (RH) near clouds (Hegg et al.,

1990). During ACE-1 Clarke et al. (1998) found that significant numbers of aerosol were being formed in the free troposphere in the outflow from convective towers. They postulated that over several days these could grow by coagulation and condensation and eventually under subsidence conditions be entrained into the MBL where they had the potential to become CCN.

Cloud processing of aerosol can significantly affect the indirect radiative forcing by aerosol. However, as cloud processing modifies the accumulation mode, the resulting particles will become more effective at directly scattering and absorbing solar radiation in cloud-free areas of the atmosphere. Thus as most atmospheric aerosol during their lifetime will be affected by cloud, cloud processing of aerosol should not be neglected when considering the evolution of aerosol spectra for direct radiative forcing investigations.

In cloudy MBLs, the cloud layer can become decoupled from the sea surface when the MBL becomes relatively deep and the turbulent mixing caused by either cloud top radiative cooling or wind shear is not enough to completely mix the MBL (Nicholls and Leighton, 1986). This causes stratification in the MBL which has implications on the evolution of aerosol in the various layers of the MBL as different processes can dominate. Decoupling was encountered extensively during ASTEX (Randall et al., 1996) and significant differences in chemistry were found between the layers. However, little regard was given to the sampling strategy to differentiate between these layers and valuable information was lost as a result (Huebert et al., 1996). In the Lagrangian experiments in ACE-2 more attention was paid to better sampling of these layers with the aircraft. In ACE-1 the experiments were biased to starting in cloud-free conditions. In ACE-2 many more experiments were carried out with extensive cloud cover to determine what cloud processing of aerosol occurs.

3. ACE-2 Lagrangian experimental strategy

The LAGRANGIAN component of ACE-2 was split up into 2 sub-projects; a cloudy air Lagrangian experiment, and a cloud-free Lagrangian experiment. The cloudy air Lagrangian experiments tracked air parcels in

the MBL between the coast of Portugal and the Canary Islands as they drifted southwest-wards in the trade winds. As they can travel up to 1000 km in 24 h, a long endurance, long range aircraft was required. Therefore the bulk of the measurements were made using the Meteorological Research Flight (MRF) C-130 air-craft which was based in Tenerife but could reach 40°N and still spend 3 or 4 h sampling the air parcel. The Research Vessel (R/V) *Vodyanitskiy*, which was also instrumented for measuring the initial aerosol and chemical characteristics of the air parcel, was positioned at the head of forecast model trajectories and then released perfluoro-carbon (PFC) tracer plumes and constant level balloons into the parcel to be tracked. The MRF C-130 aircraft was then able to follow these parcels of air for up to 36 h by making "back to back" flights out to the vicinity of the smart balloons, followed on occasion by the CIRPAS Pelican aircraft when the air parcels got close enough to the Canary Islands. Measurements were made of the aerosol physical and chemical characteristics throughout the whole depth of the MBL and the lower free troposphere during this period and the evolution of the MBL structure and cloud characteristics were closely monitored.

The cloud-free Lagrangian experiments took place at the SW tip of Portugal to take advantage of the persistent cloud-free conditions that prevail there in the summer. The main aim was to study how the aerosol characteristics of a parcel of air changed immediately after it left the continent and passed over the sea. This was done by instru-menting a ground based site at Sagres and posi-tioning the Research Vessel *Vodyanitskiy* 200 km downwind to intercept a parcel of air that had been previously characterised by Sagres to see how its aerosol had evolved. When available, the MRF C-130 aircraft flew straight and level runs at different heights between the land station and the ship to further sample how the aerosol charac-teristics evolved and to see how the thermodyn-amic and dynamic structure of the atmosphere varied in the vertical. This also allowed the aircraft to estimate how much of the continental pollution was trapped in the MBL and what was transported in the free troposphere.

3.1. ACE-2 Lagrangian operational area

The area of the Atlantic from SW Portugal, along the African coast to the SW of the Canary Islands was selected for the cloudy-air Lagrangian experiments. Climatology showed that the epi-sodic outbreaks of anthropogenic pollution effecting the Canary Islands usually came from northern Europe via the Bay of Biscay and the W of the Spanish Peninsula or from the Mediterranean via the Strait of Gibraltar. Area A in Fig. 1 indicates where the R/V *Vodyanitskiy*, the MRF C-130 and the CIRPAS Pelican operated during cloudy-air Lagrangians and area B denotes the area off Sagres where the R/V *Vodyanitskiy* and the MRF C-130 operated during the cloud-free Lagrangian experiments. These areas of the North Atlantic have the potential to be affected by 4 major aerosol types; anthropogenic aerosols from Europe and North America, mineral dust from North Africa and the Sahara, and there will always be a background of sea salt in the lowest layers of the atmosphere produced mechanically by the breaking of surface waves, and dimethyl sulphide (DMS) generated particles throughout the marine troposphere. The latter 2 will dominate in clean maritime air masses that have spent a majority of their lifetime over the central North Atlantic. ASTEX, which was conducted in the area SE of the Azores in 1992 (Albrecht et al 1995), offered an invaluable data base on MBL dynamics (Bretherton et al., 1995), cloud dynamics (Martin et al., 1995) and vertical stratification of the aerosol (Clarke et al., 1996) which was used for the planning of ACE-2 Lagrangian operations.

3.2. Participants in ACE-2 Lagrangian

The LAGRANGIAN community consists of groups from the UK, Sweden, Germany, Italy and Canada who received support from the European Union. Some participants received considerable additional support from national sources and there were several American groups who collabor-ated with the European Institutes throughout the planning and execution of the experiment. Table 1 gives a list of the contributors to ACE-2 LAGRANGIAN.

4. Lagrangian measurements

The main aim of this paper is to give a broad overview of the Lagrangian experiments and to compare and contrast the results from each. For
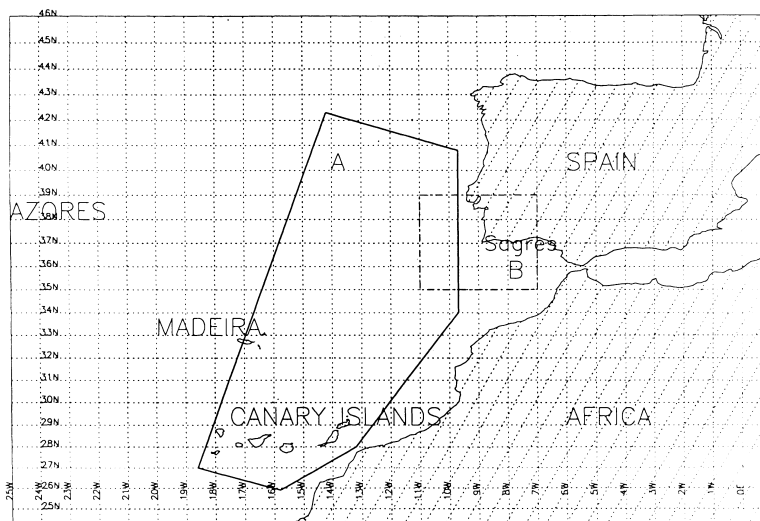
Fig. 1. Map of the area used for the ACE-2 Lagrangian experiments. Area A (surrounded by solid lines) indicates the location where the MRF C-130, R/V *Vodyanitskiy* and the CIRPAS Pelican made measurements during the cloudy air Lagrangian experiments and box B (dotted lines) around Sagres where the MRF C-130 and ship participated in the cloud-free Lagrangian experiments.

specific details about individual Lagrangian experiments the reader should refer to other papers in this issue. First, however, details are given of the items common to all the experiments such as the platforms used and the measurements made.

4.1. C-130 measurements

The instruments onboard the MRF C-130 were designed and operated by several international organisations, including MRF, University of Stockholm, Max Planck Institute, University of East Anglia, University of Sunderland, KFA, NOAA, University of Hawaii, University of York (Canada) and Brookhaven National Laboratory. They are summarised in Table 2. Information about the resolution and accuracy of the MRF instrumentation has been detailed in previous publications, notably Rogers et al. (1995) and Martin et al. (1997). New instrumentation from other European Institutes had to be fitted to the MRF C-130 to enable improved characterisation of the physical and chemical properties of the aerosol and pre-cursor gases. These are summarised below and their operating capabilities discussed.

4.1.1. Counterflow virtual impactor (MISU). A counterflow virtual impactor (CVI), (Noone et al., 1988) for collecting and analysing cloud drop residuals was installed on the C-130. The instrument payload included the CVI probe, a PMS PCASP-100 optical particle counter (OPC), a TSI 3010 condensation nuclei (CN) counter, and a bank of computer-controlled filter samplers. It has a 5 l/min sample rate and a lower cut off size of 3 μm, i.e., it collects water droplets and discards interstitial aerosol. The droplets are then evaporated and the water vapour and residual particles collected for sizing and counting and post flight chemical analysis. During ACE-2, 85 paired filter samples were collected of aerosol particles for chemical analysis and these have been analysed for major aerosol ionic species using ion chromatography.

4.1.2. VACC/SMPS system (CMAS). An instrument to provide size distributions between 10–2000 nm diameter and physico-chemical information on aerosols in the size range between 100 and 2000 nm (a VACC/SMPS system) was installed on the C-130. The fine mode size distribution was measured using a scanning/differential mobility particle sizer (S/DMPS) which had a sampling rate as high as one spectrum every 90 s and a typical size resolution of 32 channels per

Table 1. *List of main ACE-2 LAGRANGIAN participants and their contributions*

Research institute	Main scientists	Major contribution to ACE-2 LAGRANGIAN
Meteorological Research Flight, Meteorological Office, UK	Doug Johnson Simon Osborne Rob Wood Paul Field	Co-ordination of project, aircraft scientists onboard the C-130, measurement and analysis of cloud microphysics, aerosol physics and chemistry, turbulence and met. parameters
Centre for Marine and Atmospheric Science (CMAS), University of Sunderland, UK	Mike Smith Colin O'Dowd	Measurements and analysis of aerosol volatility and aerosol physics onboard the MRF C-130
MISU, Stockholm University, Sweden	Kevin Noone Paul Glantz Elisabeth Öström	Measurements and analysis of cloud particle residuals, nephelometer and soot absorption onboard the C-130
Max Planck Institute (MPI), Mainz, Germany	Meinrat O. Andreae Wolfgang Elbert Reinhart Gabriel Spyros Rapsomanikis Suzanne Hassoun	Measurements and analysis of SO_2 and DMS on board the C-130 and analysis of filter samples collected on the C-130
IFT, Leipzig, Germany and R/V *Vodyanitskiy*, NOAA PMEL, University of Washington	A. Wiedensohler D. S. Covert P. Quinn T. Bates C. Neusüb S. Philippin B. Busch D. Weise S. Henning F. Stratmann	Measurements and analysis of aerosol physics and chemistry at Sagres site and on board the R/V *Vodyanitskiy*
University of East Anglia (UEA), UK	Brian Bandy Stuart Penkett	Measurement and analysis of organic and inorganic H_2O_2 on board the C-130
Joint Research Centre, Italy University of Hawaii NOAA	Katrin Nodop Steve Businger Randy Johnson	Release of PFC and smart balloons from the ship and analysis of balloon positions
KFA, Germany	Andi Voltz-Thomas Christoph Gerbig	Measurement and analysis of CO and JNO_2 measurements onboard the C-130
York University, Canada	J. Rudolph, B. Keiser, B. Fu, and S. Fong	Hydrocarbon analysis of bottle samples collected on the C-130
Princeton University	Lynn Russell Michael Sollazzo	Entrainment rate calculations for the C-130

size decade. A PMS ASASP-X OPC was deployed inside the aircraft with this system for the accumulation mode particle sizing. Furthermore, the chemical composition of these particles was inferred using a novel high temperature, fast-response aerosol volatility analyser in conjunction with an aerosol OPC (Jennings and O'Dowd, 1990).

4.1.3. Aerosol sample inlets and mass spectrometer (MPI). Two aerosol and SO_2 isokinetic sampling probes (Andreae et al., 1988; Talbot et al., 1990) were fitted to the MRF C-130. These probes were used extensively during ACE-2 for filter sampling using specially designed filter packs. 2 sorts of samples were collected; one for the determination of water soluble components, including SO_2, and the other for organic carbon. An inertial separator was used to remove large cloud droplets and drizzle from the air stream. Both probes operated at sample flow rates of

Table 2. *A summary of the instrumentation installed on the MRF C-130 aircraft and the principal investigators involved with each measurement*

Group	Parameter	Method	Comments
MRF	temperature	Rosemount 102BL	platinum resistance
MRF	in cloud temperture	CO_2 absorption band thermometer	MRF developed
MRF	dew point	General Eastern 1011B	thermo-electric hygrometer
MRF	total water content	Lyman – α absorption hygrometer	MRF developed
MRF	wind speed and direction	Pitot static system, INU, gust probes and GPS	full corrections made for INU drift
MRF	vertical velocity	Pitot static system, INU and gust probes	
MRF	lat. and long.	GPS reciever	
MRF	altitude	radar altimeter, static pressure system	radar alt below 1525 m
MRF	cloud conditons	foward and downward facing video cameras	
MRF	liquid water content	Johnson–Williams probe	
MRF	accumulation mode aerosol spectra	PMS passive cavity aerosol spectrometer probe (PCASP)	0.1 to 3.0 μm diameter
MRF	cloud droplet spectra	PMS forward scattering spectrometer probe (FSSP)	2 to 45 μm diameter
MRF	drizzle spectra	PMS 2D-cloud probe	25 to 800 μm diameter
MRF	total CN concentrations	TSI 3025	CN > 3 nm
MRF	CCN superstauration spectra	thermal gradient diffusion chamber	MRF developed
MRF	ozone	TECO 49	UV photometric
MRF	soot absorption	radiance research particle soot absorption photometer	
MRF	aerosol scattering	TSI 3563 nephelometer	3 wavelength (450, 550, 700 nm)
MRF	broadband solar radiation	Eppley pyranometer — clear dome	0.3 to 3.0 μm
MRF	broadband solar radiation	Eppley pyranometer — red dome	0.7 to 3.0 μm
MRF	radiometric surface temp.	Heimann KT 19.82	
MISU	cloud droplet residuals	CVI inlet connected to filters, PCASP and TSI 3010	collects droplets > 3 μm
CMAS	aerosol size segragated chemistry	volatility technique. Heated chamber connected to an ASASP-X	
CMAS	fine aerosol size spectra	SMPS	100 to 2000 nm
MPI	aerosol size segregated chemistry	filter sampling; ion chromatography and organic carbon analysis	
MPI	SO_2	filter samples	
MPI	high frequency DMS	mass spectrometer	
MPI	high frequency SO_2	mass spectrometer	
UEA	organic and inorganic peroxide	fluorimetric	2 channel wet chemistry, total peroxides and organic peroxides
University of York	NMHC	bottle samples	
KFA	CO	resonance fluorescence	continuous fast response
KFA	JNO_2	UV photometer	NO_2 photolysis rate
BNL	PFC tracer detection	dual trap analyser GC	requires release of PFC tracer for plume detection
University of Hawaii	"Smart" balloon location	receiver for balloon transmissions	two-way communication between balloon and aircraft

$120 \, l \, min^{-1}$. The filter pack units consisted of 3 sequential filters (90 mm diameter) on PFA supports. The aerosol was collected on the 1st 2 filter stages (an 8.0 mm Nuclepore filter followed by a PTFE Teflon filter) which separated them into coarse ($> 1.7 \, \mu m$ diameter) and fine particles. The 3rd stage was a K_2CO_3 impregnated filter for collecting SO_2. Chemical analysis of the filters exposed during ACE-2 was performed using ion chromatography and some were selected for single particle analysis using a scanning electron microscope.

A system for fast response (20 Hz), high resolution DMS and SO_2 measurements was developed to enhance the aerosol pre-cursor gas measurements. An atmospheric pressure chemical ionization mass spectrometer (APCI-MS) was used for this purpose. To reduce losses in SO_2 an inlet was modified to be made of PFA and in line Nafion driers were installed. As only one mass spectrometer was used it was not possible to measure DMS and SO_2 simultaneously but the operation of the instrument could be altered in flight.

4.1.4. Organic and inorganic peroxides (UEA). The peroxide analyser (Penkett et al., 1995) which had previously been used on the C-130 was up-dated specifically to operate as a twin channel instrument to enable the determination of both hydrogen and organic peroxide concentrations. Peroxides are stripped from the air by passage through a stripping coil and subsequent measurement by fluorimetry. The measurement is based on the enzyme catalysed reaction between peroxides and para-hydroxy phenol acetic acid. The reaction produces water and a dimeric product, 6,6-dihydroxy-3,3-biphenyldiacetic acid which flouresces at a peak excitation wavelength of 320 nm and a peak emission wavelength of 400 nm. Peroxidase enzyme catalyses the reaction of both inorganic and organic peroxides to form the flourescent dimer and so can be used to determine the total peroxide concentration in the sample. Hydrogen peroxide vapour has a collection efficiency of 99.99% in the 10 turn stripping coil whilst organic peroxides have lower stripping efficiencies. This difference in solubility allows the determination of inorganic and organic peroxides by using a second stripping coil which collected a percentage of the remaining organic peroxides. Thus all the hydrogen peroxide and a proportion

of the organic content was determined in the first coil and organic peroxides were subsequently measured again in the second coil. In this way the hydrogen and organic peroxide concentration in the atmosphere could be determined. The instrument has a 1 Hz sampling frequency and a flow rate of $1.5 \, l \, min^{-1}$. The detection limit was 40 ± 20 pptv for hydrogen peroxide and approximately 100 ± 50 pptv for the organic measurements.

4.1.5. NMHC analysis (MRF and York University). During ACE-2, 76 bottle samples (Rudolph et al., 1998) for analysis of non-methane hydrocarbons (NMHC) were collected on the C-130 aircraft. About 100 NMHCs were determined in each of the air samples which were collected in stainless steel canisters (internally electropolished by the SUMMA process) that were cleaned, evacuated and filled with purified helium to slightly above ambient pressure. During sampling they were flushed with ambient air and then pressurised to exclude the possibility of contamination with outside air during storage. The air samples were analysed on 2 gas chromatographs, each equipped with a flame ionization detector. Many of the NMHCs were present at mixing ratios close to the lower limit of detection (about 0.3–1 ppt). The measurements were evaluated quantitatively by comparison with a calibration gas of known composition. The hydrocarbon concentrations in the calibration gas were accurate within 5%.

4.1.6. C-130 Lagrangian flights. Table 3 summarises the flights the C-130 undertook during ACE-2. In all 9 flights were carried out as part of 3 separate cloudy air Lagrangian experiments and a single flight was undertaken for the cloud-free Lagrangian experiments.

4.2. R/V Vodyanitskiy *measurements*

The R/V *Vodyanitskiy* took part in all Lagrangian experiments. Its primary aim was to identify and characterise the air parcel to be studied and then release constant level balloons and PFC tracer into it so that the aircraft could follow it. The PFC tracer was released over a 2-h period while the balloons were being filled and released.

Table 4 details the instrumentation aboard the R/V *Vodyanitskiy*. Aerosol particles were sampled

Table 3. *A list of the flights undertaken by the MRF C-130 aircraft during ACE-2*

Flight no.	Date	Flying hours	Description
A546	15/6/97	4:30	Shake down flight
A547	18/6/97	7:25	Aerosol/Stratocumulus interaction
A548	22/6/97	7:40	Island Wake effect, Pelican intercomparison
A549	25/6/97	9:10	CLOUD FREE LAGRANGIAN
A550	26/6/97	5:35	CLOUDYCOLUMN
A551	3–4/7/97	9:20	FULL LAGRANGIAN
A552	4/7/97	9:20	FULL LAGRANGIAN
A553	4–5/7/97	7:25	FULL LAGRANGIAN
A554	11/7/97	6:30	Ship intercomparison, Aerosol/Sc interaction
A555	14/7/97	4:35	Instrument test flight. Pelican intercomparison, Hidalgo intercomparison
A556	15/7/97	0:00	Ground intercomparison with Pelican
A557	16/7/97	4:20	CLOUDYCOLUMN
A558	16–17/7/97	9:25	FULL LAGRANGIAN
A559	17/7/97	8:55	FULL LAGRANGIAN
A560	17–18/7/97	9:20	FULL LAGRANGIAN
A561	18/7/97	4:05	Aerosol/Sc interaction
A562	19/7/97	5:00	CLOUDYCOLUMN
A563	20/7/97	10:00	CLEARCOLUMN over Sagres
A564	21/7/97	9:55	CLEARCOLUMN over Sagres
A565	22/7/97	9:05	CLEARCOLUMN over ship
A566	23/7/97	9:15	FULL LAGRANGIAN
A567	23–24/7/97	9:30	FULL LAGRANGIAN
A568	24/7/97	9:10	FULL LAGRANGIAN
Total hours		169:30	

at 10 m above sea level through a heated mast. The mast was capped with a rotating cone-shaped 5 cm diameter inlet that pointed into the wind and air was sampled at $1 \, m^3 \, min^{-1}$. The lower 1.5 m of the mast was heated to dry the aerosol to a RH of 55%. The aerosol was then sized every 10 min using a UDMPS (ultrafine differential mobility particle sizer), an APS (aerodynamic particle sizer), a DMPS (differential mobility particle sizer) and TSI 3010 and TSI 3025 CN counters. The UDMPS was a Vienna short column instrument connected to a TSI 3025 CN counter operating with a negative particle charge. Data were collected in 9 size bins. It operated with an aerosol flow rate of $1.5 \, l \, min^{-1}$ and a sheath air flow rate of $10 \, l \, min^{-1}$ for the first 10 days and then at $20 \, l \, min^{-1}$ for the rest of the period. The DMPS was a TSI long column instrument connected to a TSI 3010 CN counter operating with a positive particle charge. Data were collected in 17 size bins and it was operated with a flow rate of $1 \, l \, min^{-1}$ and a sheath air flow rate of $5 \, l \, min^{-1}$. The APS was a TSI 3310A. Data were collected at $1 \, l \, min^{-1}$ in size bins from 0.8 to 5.0 μm aerodynamic dia-

meter. The sample air flow was maintained at approximately 55% RH to match the sampling RH of the impactors and nephelometer.

The DMPS mobility distributions were inverted to number distributions using the inversion routine of Stratman and Wiedensohler (1997) and were corrected for diffusional losses (Covert et al., 1997) and size dependent counting efficiencies (Wiedensohler et al., 1997) based on pre-ACE-2 calibration experiments. The inverted 10 min data were averaged into 30-min periods. The APS data were converted from aerodynamic diameters to geometric diameters by dividing by the square root of the particle density. The densities were calculated using the analysed chemical mass during ACE-2 and the chemical equilibrium model AeRho (Quinn and Coffman, 1998). Further details of the instrumentation on the ship can be found in Quinn et al. (2000) and Bates et al. (2000).

4.3. Pelican measurements

The Pelican aircraft is a modified Cessna Skymaster operated by the Center for

Table 4. *A summary of the instrumentation installed on the R/V* Vodyanitskiy *aircraft and the principal investigators involved with each measurement*

Group	Parameter	Method	Comments
PMEL (Tim Bates)	Surface SW DMS	Purge and Trap. GC/SCD	
	Surface SW chlorophyl — continuous	Flourometer	excitation: 340–500 nm emission: 680 nm
	Surface SW chlorophyl — discrete	Fluorometer	excitation: 340–500 nm
	Atm. DMS	GC/SCD	
	Atm. SO_2	Pulsed fluorescence	Det limit = 50 pptv
	Particle concentration for $D > 5$ nm	UCPC	
	Particle concentration for $D > 15$ nm	CPC	
	Particle number size distribution		
	5–30 nm	UDMPS	
	20–570 nm	DMPS	
	850–5000 nm	APS	
CSIRO (John Gras)	CCN (at 0.5% supersaturation)		
PMEL (Trish Quinn)	Aerosol size segregated chemistry	Impactors	
	Major ions	IC	
	Organic and elemental carbon	Thermal analysis	
	Total mass	Gravimetry	
	Refractive index and density	Model calculations	Assume equilibrium
	Aerosol scattering coefficient	Nephelometer	450, 550, 700 nm $D < 1$ μm and $D < 10$ μm
	Aerosol backscattering coefficient	Nephelometer	450, 550, 700 nm $D < 1$ μm and $D < 10$ μm
	Aerosol absorption coefficient	PSAP	550 nm
MIM (Matthias Wiegner)	Vertical backscatter profiles	Lidar	355, 532, 1064 nm
	Cloud height		150 m to 5 km altitude for aerosol
	Aerosol layer borders		150 m to 12 km for clouds Meas. more frequent during intensive periods
NASA (Phil Russell)	Aerosol optical depth	6-channel sun tracking photometer	380, 453, 864, 1021 nm
	Column integrated ozone and H_2O		
SIO/UCSD (Robert Frouin)	Water leaving radiance	Radiometer	443, 490, 560, 670, 865 nm
	Aerosol optical depth		
	Surface SW Chlor, Phaeo Conc.		
MPI (S. Rapsomonikis)	Surface SW COS, CS_2, DMS, CH_3SH		
	Surface SW absorbance		Filtered and unfiltered samples, 200–900 nm
	Surface SW fluorescence		Filtered and unfiltered ex: 230, 254, 270, 280, 308, 323, 340, 347, 355, 370
	Surface SW pH		
	CTD profiles		
IBSS (Victor Egorov)	Surface SW temp. and salinity	Towed CTD Katran-4	
	Surface SW artificial radionuclides (^{137}Cs, ^{90}Sr, ^{239,240}Po, ^{241}Am) and natural radionuclides (^{40}K, ^{210}Pb, ^{226}Ra)	Filtration/sorption device CUNO radiochemical pre-processing	Suspended and dissolved
	Backscattering layer	Echo-sounder	SIMRAD EK-500, 38 and 120 kHz
	Surface SW PCBs, particulate and dissolved Hg		

Table 4 (cont'd)

Group	Parameter	Method	Comments
NOAA (R. Johnson)	Smart balloon releases		
JRC (Fachinetti)	Tracer releases		
PMEL (Jim Johnson)	Atmospheric T, RH, P		
	True and relative wind spd and dir		
	Surface SW temp. and salinity	TSG	
	Precipitation rate	Optical rain gauge	
	Atm. ozone		
	Atm. Rn^{222}		
	Total light intensity	Eppley	
	Vertical T, RH, P, wind spd and dir	Radiosondes	
	Ship's speed, heading, and position		
	Pitch and roll statistics		
GSF (Busch)	Aerosol growth factor	HTDMA	50, 100, 150, 250 nm dry to 55%, dry to 90%

Interdisciplinary Remotely Piloted Aircraft Studies (CIRPAS) (Bluth et al., 1996). It participated in 2 of the cloudy air Lagrangian experiments when the trajectories bought the air parcel being followed near Tenerife. Its main aim was to characterise the aerosol and measure the turbulent fluxes in the MBL and lower free troposphere. A complete description of the instrumentation on board the Pelican is given in Russell and Heintzenberg (2000).

5. Comparison of the 3 cloudy air Lagrangian experiments

3 cloudy air Lagrangian experiments were undertaken during ACE-2. The 1st between 3 and 5 July 1997, the 2nd between 16 and 18 July 1997 and the 3rd between 23 and 24 July 1997. All were remarkably different in character. Details of the measurements and initial interpretation of the results are given for (a) 1st Lagrangian in Johnson et al. (2000), (b) 2nd Lagrangian in Osborne et al. (2000), and (c) 3rd Lagrangian in Wood et al. (2000). Here an overview and comparison of the experiments are given.

5.1. Air mass trajectories

In all the cloudy air Lagrangians an anticyclone was situated to the W or N of the Azores.

However, subtle changes in the position of the axis of the ridge, which was either to the W of Ireland (as in the 1st Lagrangian) or over N Europe and the British Isles (as in the 2nd and 3rd Lagrangian), caused significant changes to the origin of the air parcel. More details of the synoptic conditions can be found in Verver et al (2000). Figs. 2–4 indicate where the air originated in the 1st, 2nd and 3rd Lagrangian, respectively. They show 4 day trajectories of air that ends up at the top of the MBL as the constant level balloon passes underneath that point. This air has the potential of being entrained into the MBL and modify the characteristics of the air parcel that is being followed. The 3D back trajectories were calculated from NCEP analyses (Draxler and Hess, 1997 – HYSPLIT4 program). The top section of each diagram shows the plan view of the trajectories and the bottom section the altitude above ground of each trajectory. Also shown are the true trajectory of the balloons and a model trajectory calculated for the altitude of the balloon.

All the trajectories in the 1st Lagrangian originated from the centre of the North Atlantic and did not pass over land in the previous 5 days; so it would be expected that the air would be relatively clean and maritime in origin. They also indicate that there was significant subsidence occurring in the free troposphere as all the trajectories came from higher up in the troposphere. The average subsidence rate calculated from these is
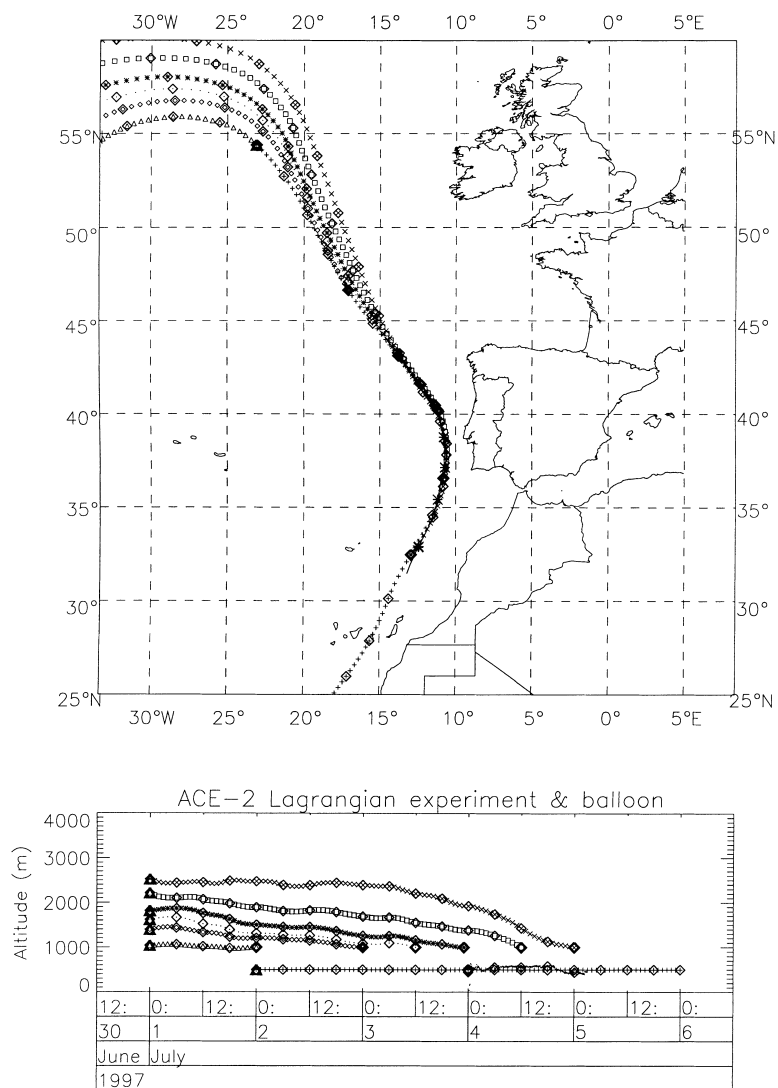
Fig. 2. Back trajectories calculated from the ECMWF model analysed fields of air that ends up at the top of the boundary layer as the air parcel being followed by the constant level balloon passes underneath during Lagrangian 1. The top diagram shows a plan view of the trajectories, the bottom diagram a side view.

0.45 cm s^{-1}. In the 2nd Lagrangian the start points for the trajectories are well scattered but they all were influenced by land. Most of the air appears to have originated near the surface over the Iberian peninsula and southern France, so the air parcel was influenced by anthropogenic pollution. The most polluted of the experiments was the 3rd Lagrangian. Here the trajectories originated over northern France and the Low Countries. This differed from the 2nd Lagrangian in that the air mass spent a lot of time over the Bay of Biscay before it reached the measurement area. Therefore, the pollution would be a day or two older than in the 2nd Lagrangian. As in the 1st Lagrangian the trajectories indicate that there was significant subsidence in the troposphere of about 0.7 cm s^{-1}.
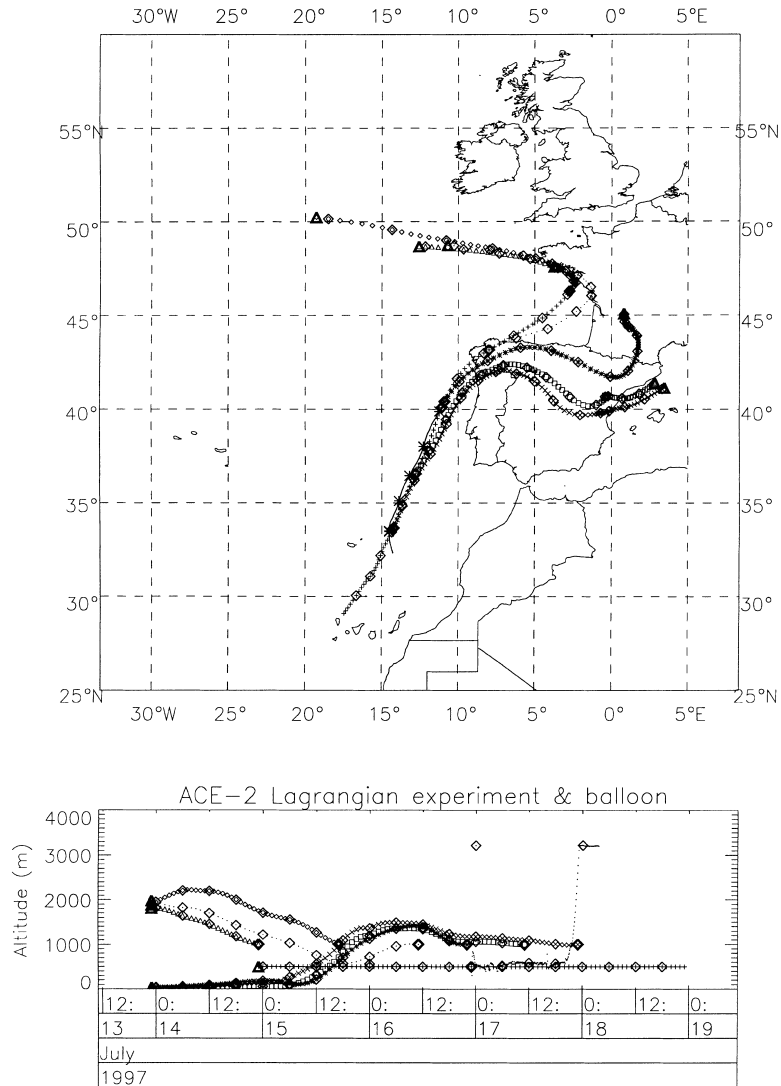
Fig. 3. Same as Fig. 6 for Lagrangian 2.

Fig. 5 shows the aircraft flight tracks superimposed on the balloon tracks for each cloudy Lagrangian. In each experiment the C-130 flew 3 flights of 9 h each separated by 3 h. In the vicinity of the balloons, profiles were flown along with box patterns at various altitudes in the MBL and the lower free troposphere which drifted with the wind 5 to 10 km behind the position of the balloons. The height of the box patterns were selected using information from the profiles so that the various layers within the MBL and lower free troposphere were well sampled. In the 1st 2 Lagrangians the CIRPAS Pelican carried out an additional flight near Tenerife. In both cases the balloons had failed by this time and the area to fly in was chosen based on extrapolated winds and forecast model trajectories. The flight patterns were used not only to characterise the MBL aerosol and chemistry but also to estimate the exchange rate of aerosol particles and gaseous
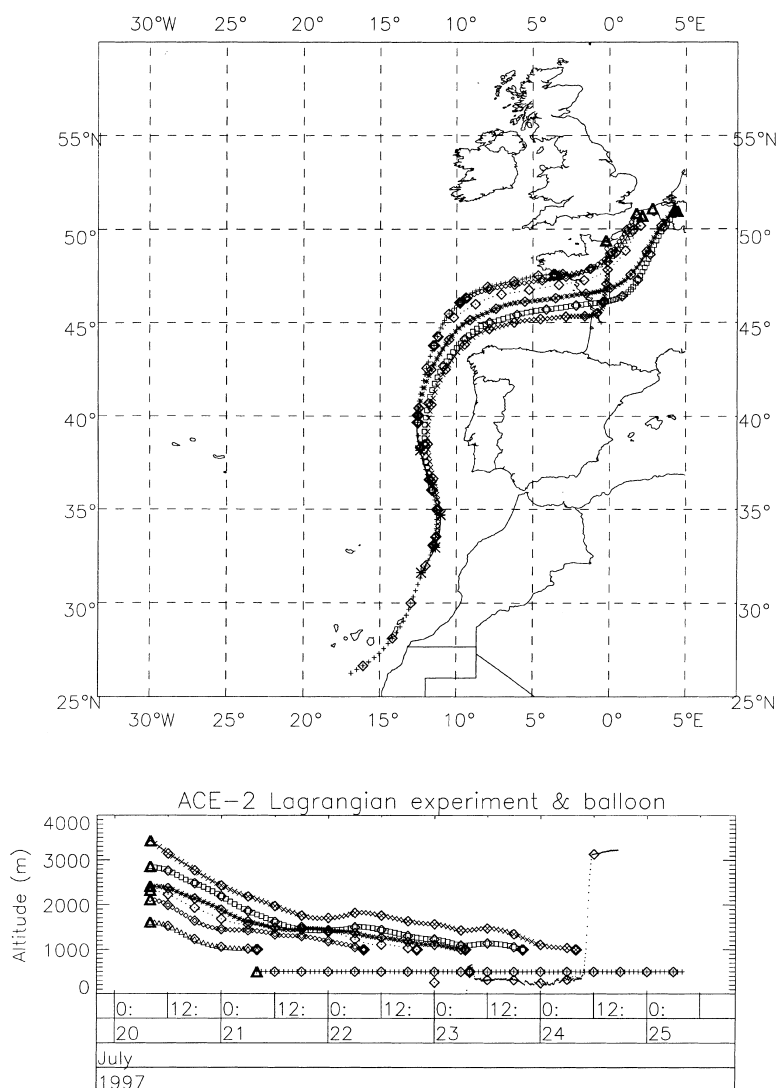
Fig. 4. Same as Fig. 6 for Lagrangian 3.

species within the MBL and with the lower free troposphere. The box patterns were chosen so that a divergence technique, based on spatially integrated horizontal winds, could be compared with an eddy correlation approach where vertical stacks of straight and level runs were used to calculate vertical fluxes. Details of these calculations can be found in Sollazzo et al. (2000). The flight patterns were also designed to map out the PFC plume released from the ship so that a mass balance of PFC could be attempted to see how fast it was

diluted with entrainment of air from the free troposphere.

5.2. *Boundary layer and aerosol evolution*

The diversity of conditions found in the 3 experiments is depicted in the schematic diagrams of the evolution of the MBL structure and general aerosol characteristics for the 1st, 2nd, and 3rd Lagrangian in Fig. 6. Also Fig. 7 shows how the accumulation mode aerosol concentrations varied
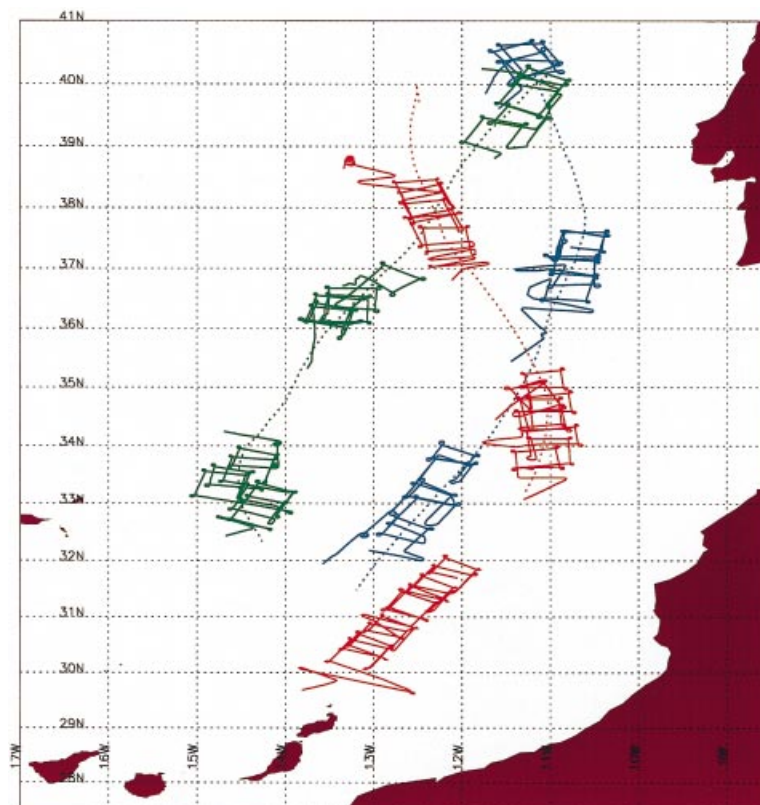
Fig. 5. Flight tracks of the C-130 for all the flights carried out in the cloudy Lagrangian experiments. The constant level balloon trajectory is indicated by the dotted line. The 1st Lagrangian are the blue lines, the 2nd Lagrangian the green lines and the 3rd Lagrangian the red lines.

in the profiles in each experiment; note the change in scale of the *x* axis in Fig. 7a compared to Fig. 7b,c required to accommodate the change from a maritime to continental air mass. The typical aerosol size spectra found in each of the experiments is shown in Fig. 8. Table 5 compares and contrasts the aerosol and meteorological conditions encountered in each cloudy Lagrangian experiment.

5.2.1. 1st Lagrangian. Even though the 1st Lagrangian experiment sampled a clean maritime air mass some surprising evolution of the aerosol characteristics was observed. The MBL started very clean but the accumulation mode concentrations increased 4-fold from 50 to 200 cm^{-3} (see Fig. 7a) in 24 h so that the MBL ended with relatively high concentrations of CCN for a clean

air mass. This was accompanied by significant changes in the MBL structure.

Initially the MBL was made up of 2 layers; a surface mixed layer (SML) and a cloud layer. Table 6 summarises the depths of the layers found. The clouds were mainly well scattered cumulus which had their base at the top of the moist SML. At times the cumulus extended up to the subsidence inversion and flattened out into broken stratocumulus layers. However, the surface wind speed increased from 7 m s^{-1} to 16 m s^{-1}. This, combined with increased surface fluxes due to the air passing over a warmer sea surface temperature, deepened the SML from 500 m to over 900 m. At the same time subsidence in the free troposphere decreased the MBL depth from 1500 m to 900 m. Therefore by the end of the experiment a well-
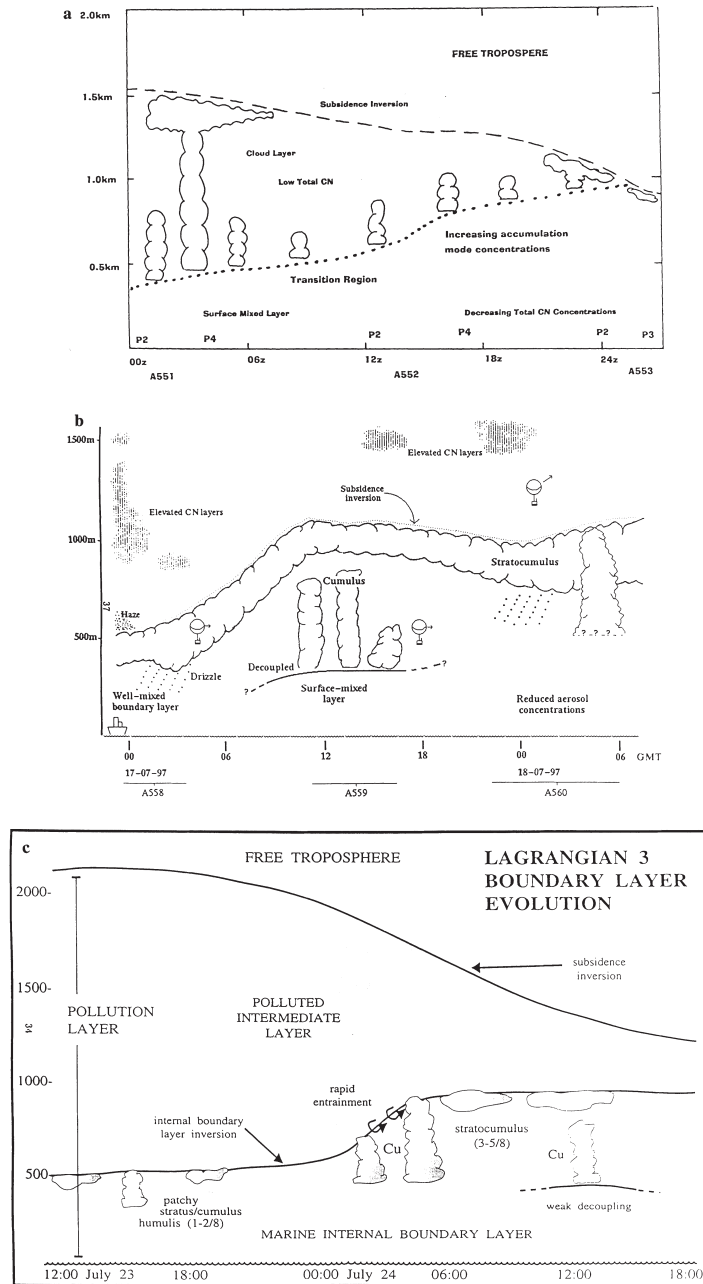
Fig. 6. Schematic diagrams of the evolution of the boundary layer and cloud structure during (a) Lagrangian 1, (b) Lagrangian 2, and (c) Lagrangian 3.
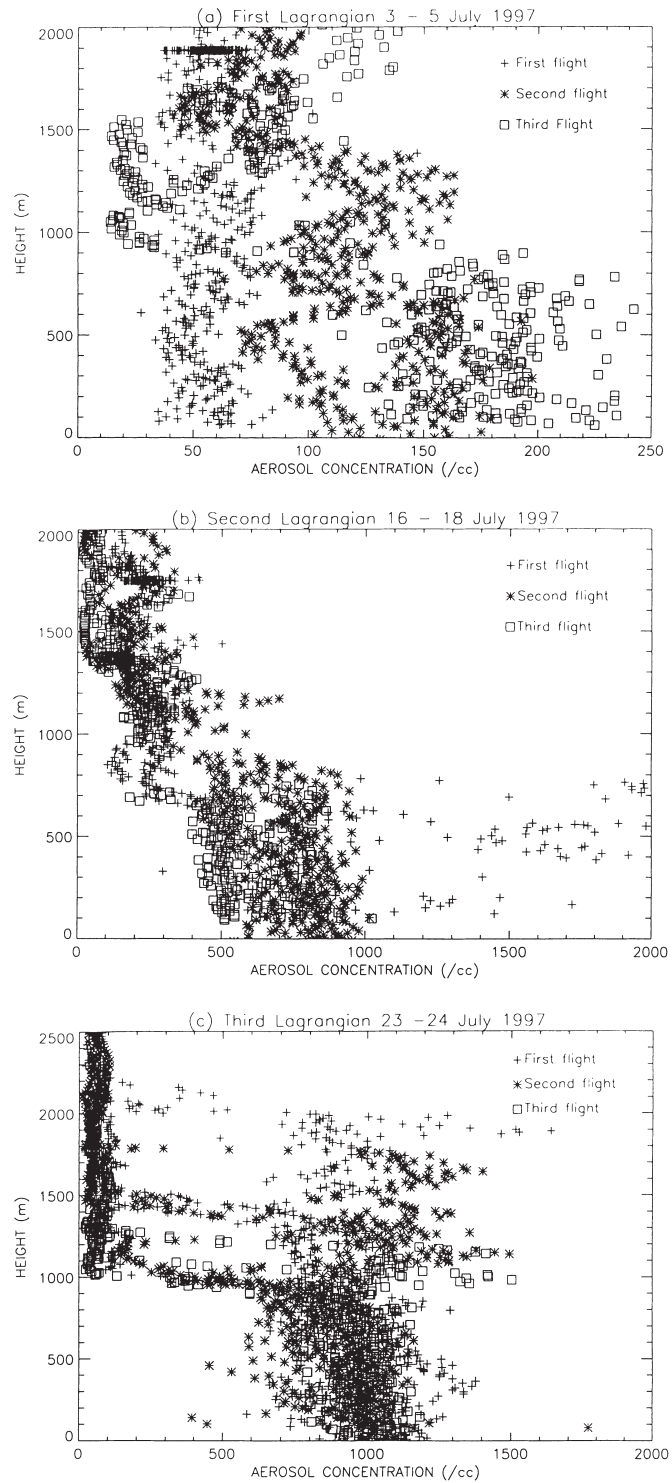
Fig. 7. A comparison of accumulation mode aerosol concentrations measured using a PCASP (0.1–3 μm diameter) by the MRF C-130 during profiles close to the constant level balloons in (a) the 1st Lagrangian (6 profiles), (b) the 2nd Lagrangian (9 profiles), and (c) the 3rd Lagrangian (9 profiles).
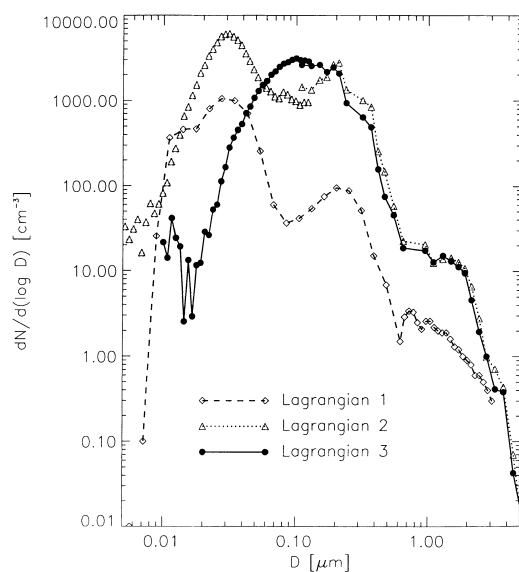
Fig. 8. A comparison of typical aerosol size spectra measured during the 1st, 2nd, and 3rd Lagrangian experiments by the ship and aircraft in the MBL.

Table 6. *A summary of the boundary layer heights during the 1st Lagrangian experiment as measured in the profiles of the MRF C-130 close to the constant level balloons*

Date	Time (GMT)	Profile	Boundary layer height (m)	Surface mixed layer height (m)
4 July 1997	00:17	P2	1570	340
4 July 1997	02:55	P4	1540	480
4 July 1997	11:40	P2	1330	670
4 July 1997	16:28	P4	1310	840
4 July 1997	22:26	P2	1130	910
5 July 1997	02:14	P3	880	880

mixed MBL was observed. The total CN concentrations had the reverse tendency to the accumulation mode concentrations. They decreased from 960 to 800 cm^{-3} in the SML and were half these values in the cloud layer.

Most of the number concentration increase in the accumulation mode was in the 0.1 to 0.4 μm diameter sizes. The reason for this is thought to

Table 5. *A comparison of the conditions found in the 1st, 2nd, and 3rd Lagrangian experiments*

	Lagragian 1	Lagragian 2	Lagragian 3
Air mass type	Clean, Maritime	Polluted from Spanish peninsula	Polluted from Northern Europe
Cloud conditions	Very scattered CU spreading out into SC	8/8 SC cover with some CU underneath	Scattered CU and SC
Total CN	1000 cm^{-3} decreasing to 800 cm^{-3}	2000 cm^{-3} to 5000 cm^{-3} decreasing to 1500 cm^{-3}	1800 cm^{-3}
Accumulation mode aerosol	50 cm^{-3} increasing to 200 cm^{-3}	600 cm^{-3} to 1800 cm^{-3} decreasing to 600 cm^{-3}	1000 cm^{-3}
Cloud droplet concentration	60 cm^{-3} increasing to 110 cm^{-3}	160 cm^{-3} to 320 cm^{-3} decreasing to 170 cm^{-3} increasing to 230 cm^{-3}	300 cm^{-3}
Drizzle	no	yes	no
Wind speed	7 m s^{-1} to 16 m s^{-1}	11 m s^{-1} to 7 m s^{-1}	10 m s^{-1} to 8 m s^{-1} to 11 m s^{-1}
Wind direction	330° to 030°	015°	340° to 020°
Sea surface temp.	292 to 295 K	293 to 295 K	293 to 295 K
Elevated pollution layers	no	yes	yes
SO$_2$	15 to 30 ppt	800 decreasing to 20 ppt	15 to 30 ppt MBL 60 to 100 ppt Pol. lay.
Ozone	30 to 40 ppb	35 to 45 ppb MBL 55 to 70 above MBL	50 to 60 ppb MBL 70 to 80 ppb Pol. lay.
H$_2$O$_2$	0.4 ppb	0.5 increasing to 1.0 ppb	0.5 ppb

be salt particle production due to the increased wind speeds (Hoell et al., 2000). The lower free troposphere was relatively clean so entrainment across the subsidence inversion is unlikely to account for the extra aerosol mass in the MBL. Some of the sulphate mass increase observed may be due to growth by direct condensation and some aqueous phase chemistry in the scattered clouds. The decrease in total CN concentration may be due to in cloud scavenging of interstitial aerosol which will enhance the number of small accumulation mode particles if they grow into the size range of the PCASP. At the beginning of the experiment where scavenging could be occurring the total CN concentrations are decreased in the cloud layer compared with the SML. Also at the end of the experiment the MBL was well mixed throughout its depth and much of the aerosol would have been passing through cloud. When this happened it was found that the total CN started to decrease throughout the depth of the MBL. The total CN values may also be decreasing due to coagulation but this seems unlikely as the time scales and the number of particles present are too small (Hoell et al., 2000).

Due to the large change in CCN characteristics in the MBL the cloud microphysics also changed significantly, with over a doubling of the cloud droplet concentration from 50 to 120 cm^{-3} and a decrease in the droplet effective radius.

5.2.2. 2nd Lagrangian. The 2nd Lagrangian was greatly different from the 1st and has provided an excellent opportunity for comparing and contrasting the processes occurring in clean air masses and polluted ones in a marine environment. In this case the MBL was polluted and continually capped by stratocumulus cloud of variable thickness in which drizzle size droplets were forming. However, it is thought that the drizzle was only reaching the surface during the first flight when the cloud base was very low.

The MBL height increased rapidly during the start of the experiment from 500 m to over 1000 m and the rapid entrainment of free tropospheric air into the MBL resulted in a measurable change to the aerosol and cloud microphysics. The air entrained initially was also polluted, as extensive pollution layers were present above the MBL. The deepening of the MBL caused the cloud layer to become decoupled from the sea surface where a SML formed. Cumuli then formed at the top of the SML and some of these penetrated the base of the stratocumulus. The heights of the pollution layer and MBL are detailed in Table 7.

Cloud processing of the aerosol was apparent. A distinct bimodal aerosol size distribution was observed (Fig. 8) in the MBL and the accumulation mode diameter showed small but measurable increases in size during the experiment. Furthermore, SO$_2$ concentrations, at 800 ppt, were relatively high at the start but decreased significantly to 40 ppt after 24 h. The sulphate fraction of the total mass of soluble aerosol in the accumulation mode also increased over the corresponding period. Overall during the experiment there was a decrease in total CN in the MBL from 5000 cm^{-3} to 1600 cm^{-3}; most of which occurred in the Aitken mode size ranges. There is strong evidence to suggest that these observations can be explained by cloud processing of the aerosol, both through aqueous phase chemistry and droplet coalescence, and dilution of the MBL with the

Table 7. *A summary of the boundary layer and pollution layer heights during the 2nd Lagrangian experiment as measured in the profiles of the MRF C-130 close to the constant level balloons*

Date	Time (GMT)	Profile	Maximum height of pollution layer (m)	Boundary layer height (m)	Surface mixed layer height (m)
16 July 1997	23:53	P2	2000	500	500
17 July 1997	01:52	P3	800	400	
17 July 1997	03:20	P4	2000	600	600
17 July 1997	10:53	P2	1200	1200	400
17 July 1997	14:40	P3	1200	1200	400
17 July 1997	16:06	P4	1200	1200	400
17 July 1997	22:29	P1	1800	1000	
18 July 1997	02:09	P2	1800	1000	
18 July 1997	04:34	P5	1200	1200	

free troposphere (Hoell et al., 2000; Dore et al., 2000). However, salt particle production, due to high surface wind speeds (10 to 11 m s^{-1}), in cloud scavenging of aerosol and vertical redistribution by drizzle may all be processes that are having significant secondary rôles.

The effect of the aerosol on the cloud microphysics in this experiment was complex. During the initial rapid entrainment event, the cloud droplet concentrations, for a short period of time, increased sharply responding to the increased accumulation mode aerosol concentrations. However, towards the end of the experiment the accumulation mode concentrations slowly decreased but the fraction activated into cloud droplets rose. Although the cloud was relatively thick throughout, coalescence of cloud droplets was suppressed as the high CCN concentrations kept cloud droplet sizes relatively small. As a result drizzle had little or no effect in washing out the pollution from the MBL. We consider that this can be generalised to most pollution outbreaks in the subtropics and that high aerosol concentrations will almost completely suppress drizzle reaching the surface and will therefore extend the lifetime of high aerosol concentrations in the MBL.

5.2.3. 3rd Lagrangian. During the 3rd Lagrangian a complex, time varying MBL was encountered. A deep, continental, pollution layer, over 2000 m deep and capped by a subsidence inversion, was observed in which a marine internal boundary layer (MIBL) grew. As there was significant subsidence in the free troposphere, the top of the pollution decreased in height to 1200 m while the MIBL rapidly grew from 500 m to 1000 m. Small cumuli grew within the MIBL and their vertical extent increased as the MIBL deepened. On occasions the cumuli spread out into well-broken stratocumulus layers at the top of the MIBL. Table 8 shows the heights of the MBL and pollution layer encountered during the aircraft profiles.

Quite remarkably though, despite the rapid changes in structure of the lower parts of the atmosphere, the aerosol characteristics displayed no change throughout the experiment. In contrast to the 2nd Lagrangian, which was also polluted, the aerosol spectra in the 3rd Lagrangian were characterised by a single, broad mode centred on 0.1 μm diameter (Fig. 8), suggesting that no cloud processing of the aerosol was going on now or in

Table 8. *A summary of the boundary layer and pollution layer heights during the 3rd Lagrangian experiment as measured in the profiles of the MRF C-130 close to the constant*

Date	Time (GMT)	Profile	Height of subsidence inversion (m)	Boundary layer height (m)
23 July 1997	11:33	P2	2100	420
23 July 1997	15:46	P3	2150	540
24 July 1997	02:19	P3	1910	795
24 July 1997	04:49	P4	1600	950
24 July 1997	10:02	P2	1520	960
24 July 1997	13:40	P3	1310	960

the recent past. The shape of the spectra and the total number concentration (between 1800 and 2000 cm^{-3} with 1000 cm^{-3} > 0.1 μm diameter) varied very little with height or time in the MIBL and most of the soluble part of the fine mode aerosol appeared to be ammonium sulphate. The aerosol was fairly aged and SO$_2$ concentrations were very low indicating that most of the gas to particle conversion had taken place prior to the measurements.

The aerosol spectra within the MBL had attained a "pseudo steady state" where either the sources and sinks of aerosol were in a fine balance or the aerosol losses were extremely small and no processing of the aerosol was going on at all. The MIBL was turbulent in nature and it was entraining air into it from a relatively quiescent layer above. But as this air was also polluted, because it was the residual of the continental boundary layer (CBL) that remained above the MIBL, it had no dilution effect on the aerosol in the MIBL. Thus the effect of entrainment of air from the clean free troposphere was minimised.

5.2.4. Inversion structure. The cloudy air Lagrangian experiments have offered an opportunity to investigate the evolution of a MBL. In each case changes to the thermodynamic structure of the layers containing the clouds have been observed and this has resulted in an evolution of the structure of the temperature inversion that caps the cloud layer. Fig. 9 shows a plot of the change in total water against the change in equivalent potential temperature across the inversion for the Lagrangian experiments. The lines on the graph define regions where mixing of air from
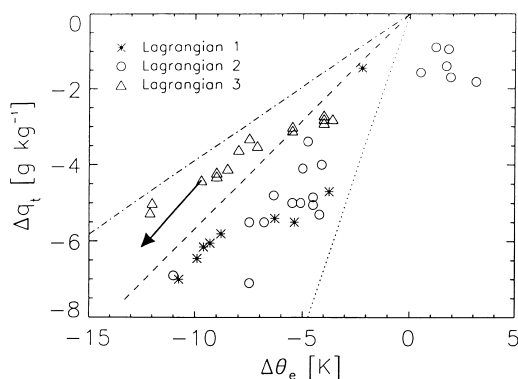
Fig. 9. A plot of the change in total water content against change in equivalent potential temperature across the inversion capping the cloud in (a) the 1st cloudy Lagrangian (stars), (b) the 2nd cloudy Lagrangian (circles) and (c) the 3rd cloudy Lagrangian (triangles).

above and below the inversion leads to either a stable result (lower right of lines) or cloud-top entrainment instability (upper left) which promotes more mixing. The dotted line indicates the cloud-top entrainment stability criterion of Deardorff et al. (1980) and Randall (1980) relevant to cases where air both above and below the inversion is saturated. The dashed line shows the criterion of MacVean and Mason (1990) for cases where the air below the inversion is saturated but the air above is subsaturated. The dash-dotted line shows the criteria for instability when neither of the layers are saturated. All the data from both the 1st and 2nd Lagrangians are stable according to the criterion of MacVean and Mason, which indicates that entrainment into the top of the clouds during these experiments would not cause an unstable condition where rapid entrainment and cloud breakup could occur. However, in the 3rd Lagrangian some of the data (to the left of the MacVean and Mason line) suggest that the presence of cloud below the inversion could lead to rapid increases in kinetic energy at the cloud top as entraining parcels of air are evaporatively cooled and become negatively buoyant.

6. Cloud-free Lagrangian experiments

3 cloud-free Lagrangian experiments were undertaken during ACE-2; 2 on 6 July and 19 July 1997 that involved the surface-based sites at Sagres

and the R/V *Vodyanitskiy*, and one on 25 June 1997 that included measurements from the MRF C-130.

6.1. Sagres site measurements

The instrument sites at Sagres were set up for the ACE-2 CLEARCOLUMN experiment and the instrumentation used there is documented in Heintzenberg and Russell (2000). There were 2 sites at Sagres; Sagres 50, at the SW tip of Portugal, and Mt. Fóia, 900 m altitude. Sagres 50 and R/V *Vodyanitskiy* had identical sets of instrumentation to determine aerosol physical (size distribution, hygroscopicity, particle number) and size segregated chemical properties (Neususs et al., 2000).

DMPS-systems were used at Sagres 50 and Mt. Fóia to measure particle size distributions in the range 3–800 nm diameter. Also, an APS was operated at Sagres 50 to determine the size distribution from 800–10 000 nm diameter. At both sites, total particle number concentrations > 3 nm were measured with an ultrafine condensation particle counter and > 10 nm with a condensation particle counter. Size distributions were obtained every 15 min and total number concentrations every minute. A volatility tandem differential mobility analyser and a hygroscopicity tandem differential mobility analyser were operated to perform continuous aerosol volatility (15 to 150 nm diameter) and hygroscopicity (35 to 250 nm diameter) measurements at the Sagres-50 site.

2, 5-stage Berner impactors (0.05–10 μm particle diameter), and 2 filter-systems were used continuously to take samples with a 12–24 h time resolution. Mass loadings and the major ions of most of the samples were determined and the absorbing aerosol fraction (Carrico et al., 2000) was measured with an Aethalometer with a time resolution of 15 min. Also, the gaseous compounds NO, NO_2, O_3, CO, and SO_2 were determined continuously with a time resolution of 1 min. In general, at the Sagres sites, it was found that particles between 0.05–1.2 μm diameter consisted mainly of $(NH_4)nH(2-n)SO_4$, whereas larger particles originated almost completely from sea-spray, where the chloride was partly replaced by nitrate (up to more than 50%). PIXE-analysis showed, that there were also low amounts of insoluble material (soil-derived) at Sagres 50.

6.2. Cloud-free Lagrangian experiment on 25 June 1997

To show an example of how the boundary layer structure and aerosol characteristics change as a polluted air mass leaves the land and enters the marine environment, the cloud-free Lagrangian experiment of 25 June 1997 is discussed. More detailed analysis of these cases will be published in future papers. The R/V *Vodyanitskiy* was positioned 200 km south of Sagres. The MRF C-130 aircraft flew profiles through the whole depth of the middle and lower troposphere over the ship and Sagres, and through the MBL into the lower free troposphere at various points between the ship and Sagres. These were then followed by box patterns at altitudes of 30 m, 500 m and 2000 m in between Sagres and the ship. Fig. 10 shows the flight track of the C-130 in the vicinity of the ship and Sagres.

As the air left the Spanish Peninsula, the surface fluxes over the relatively cool ocean and the slow subsidence in the free troposphere produced a temperature inversion close to the surface. Further away from the Sagres site this internal boundary layer or MBL started to deepen, increasing the strength of the temperature inversion. Table 9 summarises the depth of the MBL at different distances from Sagres. Over the land the surface layer was very dry. However, 200 km off the coast

Table 9. *A summary of the boundary layer heights during Lagrangian 3 as measured in the profiles of the MRF C-130 close to the constant level balloons*

Distance from Sagres (km)	Depth of boundary layer (m)	Depth of pollution layer (m)
0	no boundary layer	1600
60	83	1400
90	120	1200
190	230	1100

the layer capped by the inversion had moistened considerably. Table 9 also summarises the depth of the pollution layer measured by the aircraft at different distances from Sagres. Over Sagres enhanced concentrations of aerosol were observed up to 1600 m high, whereas over the ship the pollution layer depth had decreased to 1100 m. Fig. 11 shows the aircraft profile over the ship and Sagres of accumulation mode aerosol and total CN concentration on the left hand side, and on the right hand side a contour plot of the accumulation mode particle size spectra over the ship. Between 1100 m and 2000 m over the ship there are still remnants of the pollution that once filled a deep, convectively driven CBL, but it has been significantly diluted and in the MBL over the ship (up to a height of 230 m) the aerosol characteristics have been slightly modified. Over the ship and
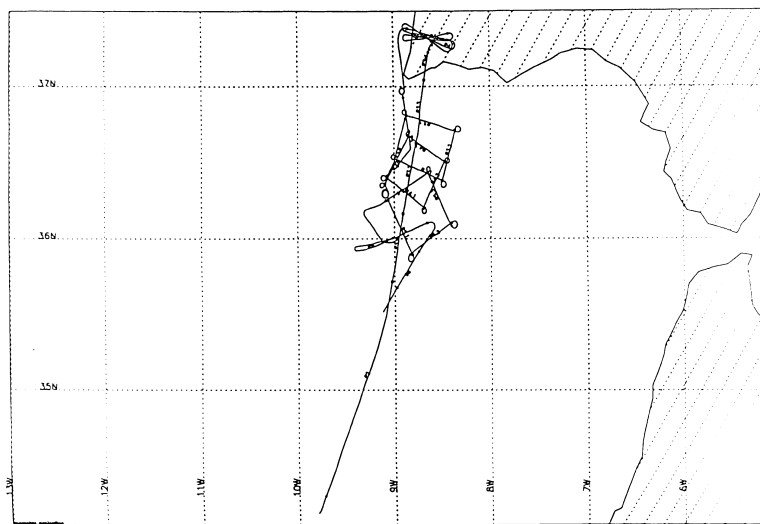

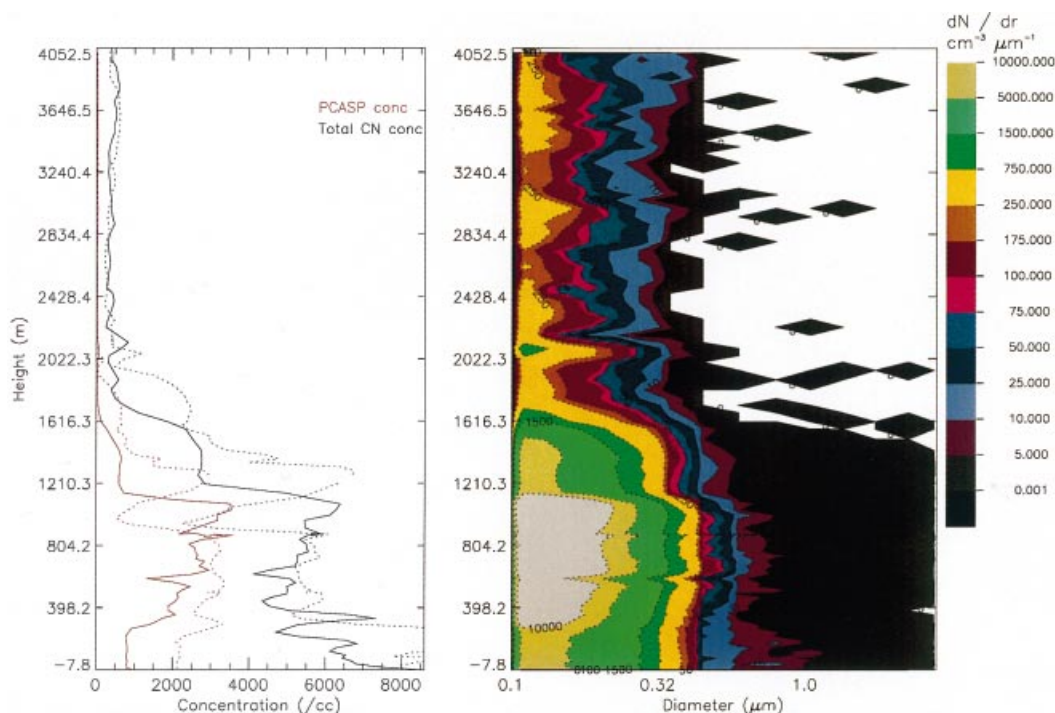*Fig. 10.* Flight track of the C-130 in the cloud-free Lagrangian on 25 June 1997.

Fig. 11. C-130 profiles of (a) accumulation mode aerosol concentrations (red) and total CN concentrations (black) (left panel) for a profile over the ship (solid line) and over Sagres (dashed line), and (b) a contour plot of accumulation mode particle size spectra over the R/V *Vodyanitskiy* during the cloud-free Lagrangian on 25 June 1997 (right panel).

over Sagres the pollution layer is characterised by accumulation mode maximum concentrations of up to 3000 cm^{-3} and total CN concentrations up to 7000 cm^{-3}, although over Sagres there are extremely high local total CN concentrations of over 15 000 cm^{-3}, which were thought to be plumes from ship stacks that the aircraft flew through. The vast majority of the increase in aerosol concentrations, compared with the free troposphere, appear to be in sizes smaller than 0.4 μm.

7. Summary and conclusions

The ACE-2 LAGRANGIAN papers presented in this issue (Johnson et al., 2000; Osborne et al., 2000; Wood et al., 2000; Sollazzo et al., 2000; Hoell et al., 2000; Dore et al., 2000) have shown that a comprehensive data set covering many case studies of the evolution of maritime and continental air masses in a marine environment have been col-

lected. As the data set produced by the ACE-2 field phase is very large and the cloud-free and cloudy air Lagrangian experiments have resulted in a wide range of different conditions being sampled it will take many years to fully analyse. We can already say that we have gone a long way in achieving objective 1 of ACE-2 which was to determine the physical and chemical character-istics of the aerosol affecting the north Atlantic region. However, the ultimate success in determin-ing the important processes in the aerosol evolu-tion can only be fully quantified once this initial analysis and interpretation of the data have been compared with the simulations and sensitivity studies of detailed process models. The data set that we have collected and is now stored in a centralised data archive at the Joint Research Center (JRC), Ispra provides a strong foundation for aerosol process modelling and parametrisation.

The 3 cloudy air Lagrangian case studies that were summarised here were all quite different in nature. The 1st Lagrangian was carried out in a

clean maritime air mass and has acted as a very good comparison with the other 2 Lagrangians which were in polluted, continental air masses. It produced the largest changes in aerosol characteristics of the 3 experiments undertaken. The quadrupling of the accumulation mode aerosol concentrations was highly correlated with the increased surface wind speeds observed and the increased salt particle production may well have acted as a sink for the sub-micron aerosol particles by enhancing coagulation. The latter, possibly, in combination with in cloud scavenging of interstitial aerosol and dilution with the free troposphere may have helped decrease the total CN concentrations in the MBL.

The 2nd Lagrangian was carried out in a polluted MBL that was completely capped by stratocumulus clouds, which was producing occasional light drizzle, but at no time reached the surface in significant quantities. SO_2 concentrations started off at relatively high levels and decreased significantly during the experiment to quite low values. This was probably due to cloud processing of the aerosol that caused a small increase in the size of the mode diameter in the accumulation mode and dilution by entrainment from the free troposphere. The effect of the entrainment of air from the free troposphere varied during the course of the experiment. Initially the air was very polluted above the MBL and the entrainment served to pollute the MBL still further. Later differential advection had replaced the pollution with cleaner air above the MBL which slowly diluted the pollution in the MBL.

In the 3rd Lagrangian dramatic changes to the thermodynamic structure of the lower atmosphere which an aged pollution layer was filling was, surprisingly, accompanied by no significant changes in the aerosol characteristics. It appears as though a deep CBL was advected out over the sea and an MIBL grew within it. Some clouds then formed at the top of the MIBL. The aerosol size spectra were remarkably constant throughout the whole of the experiment. It appeared to be in a "pseudo steady state", where either all the sources and sinks of aerosol were delicately balanced or the sources and sinks were negligible and the processing extremely slow, i.e., with time scales greater than the time period of the observations (30 h).

7.1. General description of a continental outbreak of pollution

From the analysis of the cloudy and clear air Lagrangian experiments, and information from the CLEARCOLUMN experiments, we have been able to put together a generalised description of a European continental outbreak of pollution over the sub-tropical north Atlantic. Fig. 12 shows a schematic diagram of the main features of such an event. Over the continent the surface heating in the summer months produces a deep (2 to 5 km) convectively driven CBL. The anthropogenic pollution produced over the continent is well mixed throughout the CBL. When this is advected over the relatively cold sea, the surface fluxes cause a new MBL to form which rapidly grows as the air moves away from the coast. The CBL having lost the strong surface forcing collapses under the influence of the subsidence in the free troposphere, which is generally present in the sub-tropical areas. The MBL grows within the deep pollution layer and as the top of the MBL is generally stable, a part of the pollution is trapped in a layer close to the surface. The pollution associated with the residual CBL above the top of the developing MBL will be differentially advected away as there is generally a vertical wind shear associated with the temperature inversion capping the MBL.

Eventually the subsidence in the free troposphere limits the growth of the MBL (1 to 2 km) and clean tropospheric air can be entrained into the MBL. It is this process which has the greatest effect on diluting the pollution in the MBL and assisting in evolving the continental air mass into a clean maritime air mass. Washout of the pollution by drizzle produced by clouds in the MBL is thought to be minimal, as the high levels of pollution and soluble aerosol limit the size of the cloud droplets below the size where coalescence can be effective.

The rate at which the pollution in the residual CBL is differentially advected away has a significant effect on the speed at which the dilution effect of the clean free tropospheric air can have on converting a continental air mass into a maritime air mass. If the vertical wind shear above the MBL is only small then pollution layers above the MBL can be entrained into the top of the MBL topping up the aerosol there and thus maintaining the
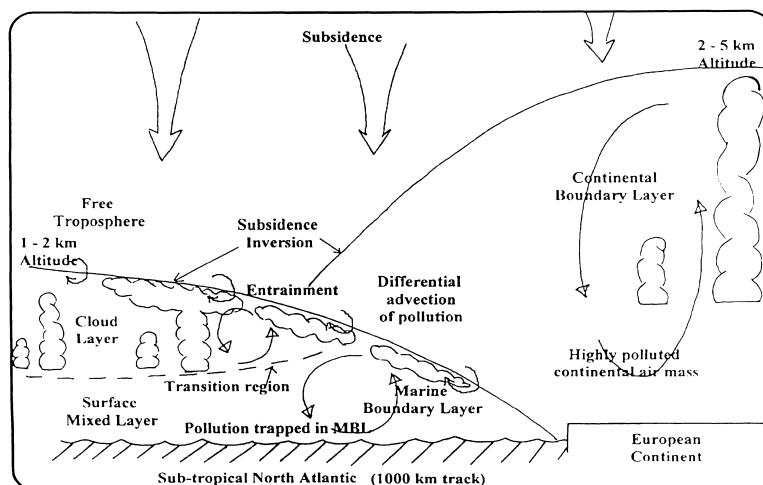
Fig. 12. A generalised picture of a European outbreak of pollution over the sub-tropical North Atlantic.

continental air mass for longer than would be expected. This was evidently true in the 3rd cloudy air Lagrangian where the air had been over the sea for over 2 days but very little evolution of the aerosol in the MBL was going on as the residual CBL was still present above the top of the MBL. In contrast, in the 2nd cloudy air Lagrangian the air had only been over the sea for half a day but the pollution in the residual CBL was advected away relatively quickly and so entrainment of clean free tropospheric air could begin to have a significant effect on the evolution of the aerosol in the MBL.

The evolution of the MBL also has a modifying effect on the evolution of the aerosol characteristics. As the air moves over progressively warmer seas the MBL deepens and moisture builds up and stratocumulus clouds form at the top of the MBL. If the MBL gets deep enough then the generation of turbulent kinetic energy, either by wind shear or cloud top cooling, may not be enough to maintain a well-mixed MBL. The cloud layer then becomes decoupled from the moisture source at the surface. The MBL then becomes layered with a surface mixed layer (SML) and a layer containing the cloud. Moisture builds up in the SML and it becomes conditionally unstable and cumulus clouds will grow from the top of the SML and these will help maintain the stratocumulus layer by locally supplying it with moisture. The cycling of the aerosol through this cloud will process it either through: (a) aqueous phase chemical reactions which will increase the mean size of the aerosol through sulphate production, (b) coalescence of cloud droplets which will decrease the aerosol number concentration and increase the aerosol mean size, and (c) scavenging of interstitial aerosol by the cloud droplets which will decrease the total CN concentrations and increase the aerosol mean size. All of these processes will tend to enhance the accumulation mode, which will firstly, improve the CCN characteristics of the aerosol, and secondly modify the direct radiative forcing effect of the aerosol as the aerosol size becomes more comparable with the wavelength of light which will increase its light scattering capabilities.

The total length of time the aircraft were able to track the parcels of air in the Lagrangian experiments was not enough to examine the complete evolution from a continental to a maritime air mass. Modelling studies by Fitzgerald et al. (1998) suggest that the time scale of this is about 6 to 8 days. However, these experiments do show how important cloud processing and entrainment are in modifying the aerosol size spectrum in the MBL as suggested by Clarke et al. (1998), Russell et al. (1998), Van Dingenen et al. (1999) and Fitzgerald et al. (1998). The aerosol size spectra in the 2nd and 3rd cloudy air Lagrangian experiments were quite different in nature, one being bi-modal due to recent/continuing cloud processing and the other uni-modal due to a limited interaction with clouds. In the 3rd Lagrangian experiment if cloud

processing of the aerosol has taken place prior to the measurements then more recent dilution with the pollution layer above the MBL has filled in the cloud processing minimum in the aerosol spectra. The time constant for doing this is typically around 2 days (Fitzgerald et al., 1998).

Recent observations during ACE-1 (Clarke et al., 1998; Russell et al., 1998) and modelling studies (Van Dingenen et al., 1999; Fitzgerald et al., 1998) have indicated the importance of entrainment and dilution of the MBL air with free tropospheric air. By its very nature it is a very slow process, so at times, even in remote marine areas, its effects can be swamped by stronger more effective processes. This was certainly the case in the 1st cloudy Lagrangian experiment where the synoptic pressure gradient strengthened, increasing the wind speed, and resulting in a significant source of new particles at the surface which dominated entrainment processes and the evolution of the MBL aerosol characteristics. At times, at the start of the 2nd cloudy Lagrangian and throughout the whole period of the 3rd cloudy Lagrangian, entrainment of polluted air from above the top of the MBL maintained the pollution characteristics of the MBL. In the 3rd Lagrangian, as the aerosol above the MBL had virtually the same characteristics as the aerosol in the MBL this caused no modification of the aerosol size spectra at all.

Homogeneous nucleation is a not well understood. Clear correlations between new particle formation events and pre-cursor gases, meteorology, and other aerosol properties such as surface area have not been clearly determined. Weber et al. (1995) found indications that with increasing sulphuric acid concentrations in the gas phase, particle formation is enhanced. Birmili (1998) and Birmili and Wiedensohler (1998) found at a polluted rural site in Germany frequent new particle formation events of $20\,000$–$200\,000$ cm^{-3} over several hours in the morning (on average every tenth day). However, in none of the cloudy Lagrangian experiments was there any evidence of new particle formation in the MBL. At Sagres, though, every second day new particle formation was found in the morning hours, and every fifth day, a growth of the nucleation mode into the Aitken mode was observed indicating that the new particle formation took place regionally and was not caused by local point sources or ships.

7.2. Development of parametrisations of aerosol processes

If the data are to have a major impact on the reliability of climate model predictions then improved parametrisations of aerosol processes have to be developed for large-scale numerical model physics packages. Due to the wide diversity of conditions encountered during the Lagrangian experiments an ideal platform for parametrisation development is now available. The ultimate aim of this work will be to develop improved parametrisations of aerosol processes in order that objective 3 of ACE-2 can be fulfilled, i.e., to determine the regional direct and indirect radiative forcing of aerosols in the North Atlantic region. Work is currently being undertaken in collaboration with the UK Meteorological Office Hadley Centre and the ECHAM modeling community in validating and improving aerosol parametrisations for large scale numerical models. An example of a parametrisation of a GCM sulphur cycle scheme that is being worked on is shown in Fig. 13. The aerosol is split up into 3 modes; a dissolved sulphate mode, an accumulation sulphate mode and an Aitken sulphate mode. The sources and sinks of mass for these 3 modes are shown in the
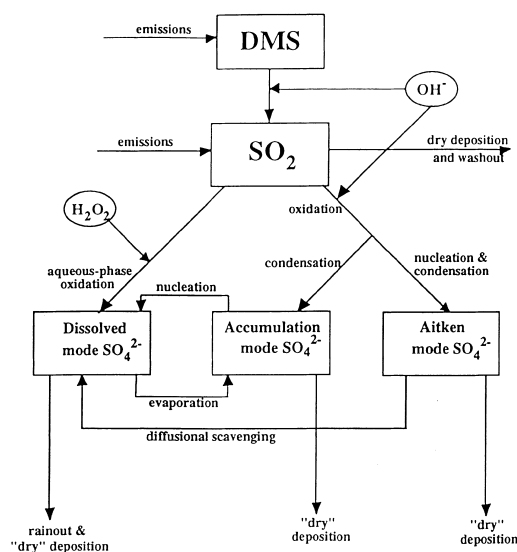

Fig. 13. A schematic diagram of the parametrisation of the sulphur cycle proposed for the Unified Model used in the UK Met. Office (Courtesy of Dr. D. L. Roberts, Hadley Centre).

diagram. A similar aerosol scheme for nitrates could also be devised. The data set that has been collected for ACE-2 LAGRANGIAN will help considerably in determining how best to represent the movement of mass from one mode to another in such a scheme but this will only be possible once the important processes have been fully understood. Untangling the complex nature of the different processes that are present in these different Lagrangian experiments to modify the aerosol evolution will keep modellers and experimental physicists busy for many years to come.

8. Acknowledgements

REFERENCES

Albrecht, B. A., Bretherton, C. S., Johnson, D. W., Schubert, W. H. and Frisch, A. S. 1995. The Atlantic Stratocumulus Transition Experiment – ASTEX. *Bull. Amer. Met. Soc.* **76**, 889–904.

Andreae, M. O., Berresheim, H., Andreae, T. W., Kritz, M. A., Bates, T. S. and Merril, J. T. 1988. Vertical distribution of dimethylsulfide, sulfur dioxide, aerosol ions and radon over the north east Pacific Ocean. *J. Atmos. Chem.* **6**, 149–173.

Bates, T. S., Huebert, B. J., Gras, J. L., Griffiths, F. B. and Durkee, P. A. 1998. International Global Atmospheric Chemistry (IGAC) Project's First Aerosol Characterization Experiment (ACE-1): overview. *J. Geophys. Res.* **103**, 16,297–16,318.

Bates, T. S., Quinn, P. K., Covert, D. S., Coffman, D. J., Johnson, J. E. and Wiedensohler, A. 2000. Aerosol physical properties and controlling processes in the lower marine boundary layer: a comparison of submicron data from ACE-1 and ACE-2. *Tellus* **52B**, 258–272.

Benkovitz, C. M., Berkovitz, C. M., Easter, R. C., Nemesure, S., Wagener, R. and Schwartz, S. E. 1994. Sulphate over the North Atlantic and adjacent continental regions: evaluation for October and November 1986 using a three-dimensional model driven by observation derived meteorology. *J. Geophys. Res.* **99**, 20,725–20,756.

Birmili, W. 1998. *Production of new ultrafine aerosol particles in continental air mass.* PhD thesis, University of Leipzig, Germany.

Birmili, W. and Wiedensohler, A. 1998. The influence of meteorological parameters on ultrafine particle production at a continental site. *J. Aerosol. Sci.* **29**, S1015–1016.

Bluth, R. T., Durkee, P. A., Seinfeld, J. H., Flagan, R. C., Russell, L. M., Crowley, P. A. and Finn, P. 1996. Center for Interdisciplinary Remotely-Piloted Aircraft Studies (CIRPAS). *Bulletin of the American Met. Soc.* **77**, 2691–2699.

Bower, K., Choularton, T. W., Gallagher, M. W., Beswick, K. M., Flynn, M., Allen, A. G., Davison, B. M., James, J. D., Robertson, L., Harrison, R. M., Hewitt, C. N., Cape, J. N., McFadyen, G. G., Martinsson, B. G., Frank, G., Swietlicki, E., Zhou, J., Berg, O. H., Mentes, B., Papaspiroulos, G., Hansson, H.-C., Kulmala, M., Aalto, P., Vakeva, M., Berner, A., Bizjak, M., Fuzzi, S., Laj, P., Facchini, M.-C., Orsi, G., Ricci, L., Nielsen, M., Allan, B. J., Coe, H., McFiggans, G., Plane, J. M. C., Collett Jr., J. L., Moore, K. F. and Sherman, D. E. 2000. ACE-2 HILLCLOUD: an overview of the ACE-2 ground based cloud experiment. *Tellus* **52B**, 750–778.

Bretherton, C. S, Austin, P. and Siems, S. T. 1995. Cloudi-

ness and marine boundary layer dynamics in the ASTEX Lagrangian experiments. Part II: cloudiness, drizzle, surface fluxes and entrainment. *J. Atmos. Sci.* **52**, 16, 2707–2723.

Businger, S., Chiswell, S. R., Ulmer, W. C. and Johnson, R. 1996. Balloons as a Lagrangian measurement platform for atmospheric research. *J. Geophys. Res.* **101**, 4363–4376.

Businger, S., Johnson, R., Katzfey, J., Siems, S. and Wang, O. 1999. Smart Tetroons for Lagrangian air-mass tracking during ACE-1. *J. Geophys. Res.* **104**, 11,709–11,722.

Carrico, C. M., Rood, M. J., Ogren, J., Neusüss, C., Wiedensohler, A. and Heintzenburg, J. 2000. Aerosol optical properties at Sagres, Portugal during ACE-2. *Tellus* **52B**, 694–715.

Charlson, R. J., Lovelock, J. E., Andreae, M. O. and Warren, S. G. 1987. Oceanic phytoplankton, atmospheric sulfur, cloud albedo and climate. *Nature* **326**, 655–661.

Charlson, R. J., Langner, J., Rodhe, H., Levoy, C. B. and Warren, S. G. 1991. Perturbation of the northern hemisphere radiative balance by backscattering from anthropogenic sulfate aerosols. *Tellus* **43A/B**, 152–163.

Clarke, A. D., Uehara, T. and Porter, J. N. 1996. Lagrangian evolution of an aerosol column during the Atlantic Stratocumulus Transition Experiment. *J. Geophys. Res.* **101**, 4351–4362.

Clarke, A. D., Varner, J. L., Eisele, F., Mauldin, R. L, Tanner, D. and Litchy, M. 1998. Particle production in the remote marine atmosphere: cloud outflow and subsidence during ACE-1. *J. Geophys. Res.* **103**, 16,397–16,409.

Covert, D. S., Kapustin, V. N., Quinn, P. K. and Bates, T. S. 1992. New particle formation in the marine boundary layer. *J. Geophys. Res.* **92**, 20,581–20,589.

Covert, D., Wiedensohler, A. and Russell, L. M. 1997. Particle charging and transmission efficiencies of aerosol charge neutralizers. *Aerosol Sci. and Technol.* **27**, 206–214.

Deardorff, J. W., Willis, G. E. and Stockton, B. H. 1980. Laboratory studies of the entrainment zone of a convectively mixed layer. *J. Fluid Mech.* **100**, 41–46.

Dore, A., Johnson, D. W., Osborne, S., Choularton, T., Bower, K., Andreae, M. O. and Bandy, B. 2000. The evolution of boundary layer aerosol particles due to in-cloud chemical reactions during the second Lagrangian experiment of ACE-2. *Tellus* **52B**, 452–463.

Draxler, R. R. and Hess, G. D. 1997. *Description of hysplit 4 modelling*. Technical Memorandum ERL ARL-224, NOAA.

Fiengold, G., Kreidenweiss, S. M., Stevens, B. and Cotton, W. R. 1996. Numerical simulations of stratocumulus processing of cloud condensation nuclei through collision coalescence. *J. Geophys. Res.* **101**, 21,391–21,402.

Fitzgerald, J. W., Marti, J. J., Hoppel, W. A., Frick, G. M. and Gelbard, F. 1998. A one dimensional sectional model to simulate multicomponent aerosol dynamics in the marine boundary layer (2). Model application. *J. Geophys. Res.* **103**, 16,103–16,117.

Hegg, D. A. 1985. The importance of liquid phase oxidation of SO_2 in the troposphere. *J. Geophys. Res.* **90**, 373–3779.

Hegg, D. A., Radke, L. F. and Hobbs, P. V. 1990. Particle production associated with marine clouds. *J. Geophys. Res.* **95**, 13,917–13,925.

Hoell, C., O'Dowd, C., Johnson, D. W., Osborne, S. R. and Wood, R. 2000. Timescale analysis of marine boundary layer aerosol evolution: Lagrangian case studies under clean and polluted conditions. *Tellus* **52B**, 423–438.

Huebert, B. J., Pszenny, A. and Blomquist, B. 1996. The ASTEX/MAGE experiment. *J. Geophys. Res.* **101**, 4319–4329.

IPCC, 1995. Climate Change 1995. The science of climate change. Contribution of WG1 to the second assessment Report of the Intergovernmental Panel on Climate Change (eds. Houghton, J. T., Meira Filho, L. G., Callender, B. A., Harris, N., Kattenberg, A and Maskell, K.). Cambridge University Press.

Jennings, S. G. and O'Dowd, C. 1990. Volatility of aerosol at Mace Head on the West coast of Irelan. *J. Geophys. Res.* **95**, 13,937–13,948.

Johnson, D. W., Osborne, S., Wood, R., Suhre, K., Quinn, P. K., Bates, T. S., Andreae, M. O., Noone, K., Glantz, P., Bandy, B., Rudolph, J. and O'Dowd, C. 2000. Observations of the evolution of the aerosol, cloud, and boundary layer characteristics during the first ACE-2 Lagrangian experiment. *Tellus* **52B**, 348–374.

Johnson, R., Businger, S. and Baerman, A. 2000. Lagrangian air mass tracking with smart balloons during ACE-2. *Tellus* **52B**, 321–334.

Kiehl, J. T. and Briegleb, B. P. 1993. The relative roles of sulfate aerosols and greenhouse gases in climate forcing. *Science* **260**, 311–314.

Kiehl, J. T. and Rodhe, H. 1995. Modelling geographical and seasonal forcing due to aerosols. In: *Aerosol forcing of climate* (eds. Charlson, R. and Heintzenberg, J.). Wiley Interscience.

Langner, J. and Rodhe, H. 1991. A global three-dimensional model of the tropospheric sulfur cycle. *J. Atmos. Chem.* **13**, 225–263.

Martin, G. M., Johnson, D. W., Rogers, D. P., Jonas, P. R., Minnis, P. and Hegg, D. 1995. Observations of the interaction between cumulus clouds and warm stratocumulus clouds in the marine boundary layer during ASTEX. *J. Atmos. Sci.* **52**, 2902–2922.

Martin, G. M., Johnson, D. W., Jonas, P. R., Rogers, D. P. and Brooks, I. M. 1997. Effects of airmass type on the interaction between cumulus clouds and warm stratocumulus clouds in the marine boundary layer. *Quart. J. Roy. Meteor. Soc.* **123**, 849–882.

McVean, M. K. and Mason, P. J., 1990. Cloud top entrainment instability through small scale mixing and

its parametrisation in numerical models. *J. Atmos. Sci.* **47**, 1012–1030.

Murphy, D. M., Anderson, J. R., Quinn, P. K., McInnes, L. M., Brechtel, F. J., Kreidenweis, S. M., Middlebrook, A. M., Posfai, M., Thomson, D. S. and Buseck, P. R. 1998. Influence of sea salt on aerosol radiative properties in the Southern Ocean marine boundary layer. *Nature* **392**, 62–65.

Neusüss, C., Weise, D., Birmili, W., Wex, H., Wiedensohler, A. and Covert, D. 2000. Size-segregated chemical, gravimetric and number distribution derived mass closure of the aerosol in Sagres, Portugal during ACE-2. *Tellus* **52B**, 169–184.

Nicholls, S. and Leighton, J. 1986. An observational study of the structure of stratiform cloud sheets. Part I: structure. *Quart. J. Roy. Meteor. Soc.* **112**, 431–460.

Noone, K. J., Ogren, J. A., Heintzenberg, J., Charlson, R. J. and Covert, D. S. 1988. Design and calibration of a counterflow virtual impactor for sampling of atmospheric fog and cloud droplets. *Aerosol Sci. and Technol.* **8**, 235–244.

O'Dowd, C. D. and Smith, M. H. 1993. Physiochemical properties of aerosols over the Northeast Atlantic: evidence for wind speed related submicron sea salt aerosol production. *J. Geophys. Res.* **98**, 1137–1149.

Osborne, S. R., Johnson, D. W., Wood, R., Bandy, B. J., Andreae, M. O., O'Dowd, C., Glantz, P., Noone, K., Rudolf, J., Bates, T. and Quinn, P. 2000. Observations of the evolution of the aerosol, cloud and boundary layer dynamic and thermodynamic characteristics during the second Lagrangian experiment of ACE-2. *Tellus* **52B**, 375–400.

Pandis, S. N., Russell, L. M. and Seinfeld, J. H. 1994. The relationship between DMS flux and CCN concentration in remote marine regions. *J. Geophys. Res.* **99**, D8, 16,945–16,957.

Penkett, S. A., Bandy, B. J., Reeves, C. E., McKenna, D. and Hignett, P. 1995. Measurements of peroxides in the atmosphere and their relevance to the understanding of global tropospheric chemistry. *Faraday Discussions* **100**, 155–174.

Penner, J. E., Charlson, R. J., Hales, J. M., Laulainen, N., Leifer, R., Novakov, T., Ogren, J., Radke, L. F., Schwartz, S. E. and Travis, L. 1994. Quantifying and minimizing uncertainty of climate forcing by anthropogenic aerosol. *Bull. Amer. Met. Soc.* **75**, 375–400.

Quinn, P. K. and Coffman, D. J. 1998. Local closure during the First Aerosol Characterization Experiment (ACE-1): aerosol mass concentration and scattering and backscattering coefficients. *J. Geophys. Res.* **103**, 16,575–16,596.

Quinn, P. K., Bates, T. S., Coffman, D. J., Miller, T. L. and Johnson, J. E. 2000. A comparison of aerosol chemical and optical properties from the first and second aerosol characterisation experiments. *Tellus* **52B**, 239–257.

Raes, F. 1995. Entrainment of free tropospheric aerosols as a regulating mechanism for cloud condensation nuclei in the remote marine boundary layer. *J. Geophys. Res.* **100**, 2893–2903.

Raes, F., Bates, T., Verver, G., McGovern, F.and Van Liedekerke, M. 2000. The second aerosol characterisation experiment (ACE-2): general context and main results. *Tellus* **52B**, 111–126.

Randall, D. A. 1980. Conditional instability of the first kind upside down. *J. Atmos. Sci.* **37**, 125–130.

Randall, D. A., Albrecht, B., Cox, S., Johnson, D. W., Minnis, P., Rossow, W. and Starr, D. O'C. 1996. On FIRE at ten. *Advances in Geophysics* **38**. Academic Press.

Rogers, D. P., Johnson, D. W. and Friehe, C. A. 1995. The stable internal boundary layer over a coastal sea (I). Airborne measurements of the mean and turbulence structure. *J. Atmos. Sci.* **52**, 667–683.

Rudolph, J., Kieser, B., Fu, B. and Fong. S. 1998. *Hydrocarbon measurements during ACE-2.* University of York report.

Russell, P. B. and Heintzenberg, J. 2000. An overview of the ACE-2 clear sky column closure experiment (CLEARCOLUMN). *Tellus* **52B**, 463–483.

Russell, L. M., Lenschow, D. H., Laursen, K. K., Krummel, P. B., Siems, S. T., Bandy, A. R., Thornton, D. C. and Bates, T. S. 1998. Bidirectional mixing in an ACE-1 marine boundary layer overlain by a second turbulent layer. *J. Geophys. Res.* **103**, 16,411–16,432.

Sievering, H., Boatman, J., Gorman, E., Kim, Y., Anderson, L., Ennis, G., Luria, M. and Pandis, S. 1992. Removal of sulfur from the marine boundary layer by ozone oxidation in sea salt aerosols. *Nature* **360**, 571–573.

Sollazzo, M. J., Russell, L. M., Percival, D., Osborne, S., Wood, R. and Johnson, D. W. 2000. Entrainment rates during ACE-2 Lagrangian experiments calculated from aircraft measurements. *Tellus* **52B**, 335–347.

Stratman, F. and Wiedensohler, A. 1997. A new data inversion algorithm for DMPS measurements. *J. Aerosol Sci.* **27**, S1, 339–340.

Suhre, K., Andreae, M. O. and Rosset, R. 1995. Biogenic sulfur emissions and aerosols over the tropical South Atlantic (2). One dimensional simulation of sulfur chemistry in the marine boundary layer. *J. Geophys. Res.* **100**, 11,323–11,334.

Talbot, R. W., Andreae, M. O., Berresheim, H., Artaxo, P., Garstang, M., Harriss, R. C., Beecher, K. M., and Li, S. M. 1990. Aerosol chemistry during the wet season in central Amazonia: the influence of long range transport. *J. Geophys. Res.* **95**, 16,955–16,969.

Van Dingenen, R., Raes, F., Putaud, J.-P., Virkkula, A. and Mangoni, M. 1999. Processes determining the relationship between aerosol number and non-sea-salt sulphate mass concentrations in the clean and perturbed marine boundary layer. *J. Geophys. Res.* **104**, 8027–8038.

Verver., G., Raes, F., Vogelezang, D. and Johnson, D. 2000. The second aerosol characterisation experiment

(ACE-2): meteorological and chemical context. *Tellus* **52B**, 126–140.

Weber, R. J., McMurry, P. H., Eisele, F. L. and Tanner, D. J. 1995. Measurement of expected nucleation precursor species and 3 to 500 nm diameter particles at Mauna Loa Observatory, Hawaii. *J. Atmos. Sci.* **12**, 2242–2257.

Wiedensohler, A., Orsini, D., Covert, D. S., Coffmann, D., Cantrell, W., Havlicek, M., Brechtel, F. J., Russell, L. M., Weber, R. J., Gras, J., Hudson, J. G. and Litchy, M. 1997. Intercomparison study of size

dependent counting efficiency of 26 condensation particle counters. *Aerosol Sci. and Technol.* **27**, 224–242.

Wood, R., Johnson, D. W., Osborne, S. R., Bandy, B. J., Andreae, M. O., O'Dowd, C., Glantz, P. and Noone, K. J. 2000. Boundary layer, aerosol and chemical evolution during the third Lagrangian experiment of ACE-2. *Tellus* **52B**, 401–422.

Zhuang, L. and Huebert, B. J. 1996. A Lagrangian analysis of the total ammonia budget during ASTEX/MAGE. *J. Geophys. Res.* **101**, 4341–4350.